Constraining the Hadron-Quark Phase Transition Chemical Potential via Astronomical Observations

Zhan Bai(摆展)
Peking University

May 9th, 2019
Continuum Fnctional Methods for QCD at New Generation Facilities
Trento, Italy

OUTLINE

1. Introduction and Motivation
2. Constructing Hadron-Quark Phase Transition
3. Hadron Model and Quark Model
4. Numerical Results
5. Summary

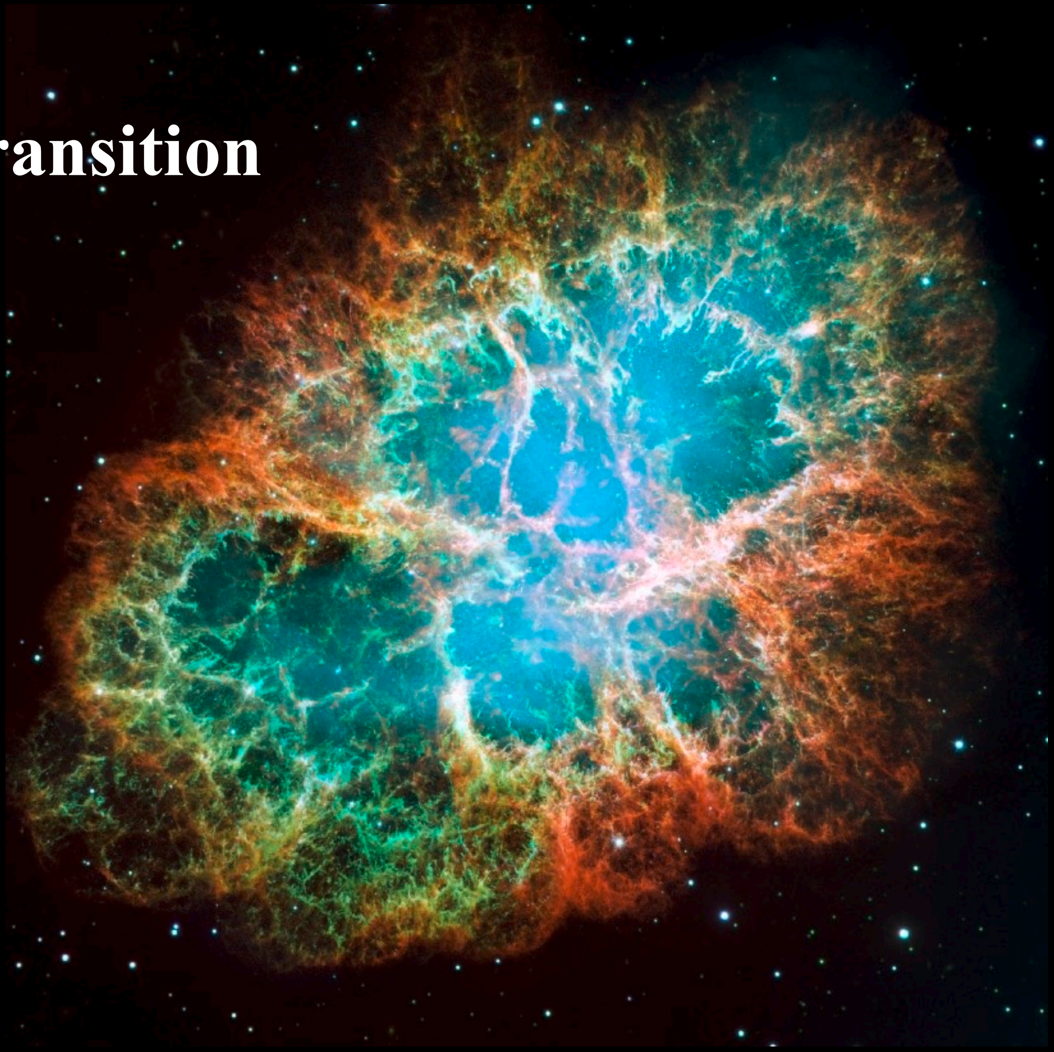

1. INTRODUCTION

• Exploring the phase structure of quantum chromodynamics (QCD) has long been one of the most interesting topics in the field of strong interaction physics, and the condition for which quark and gluon become deconfined is essential in the study of QCD phase structure.

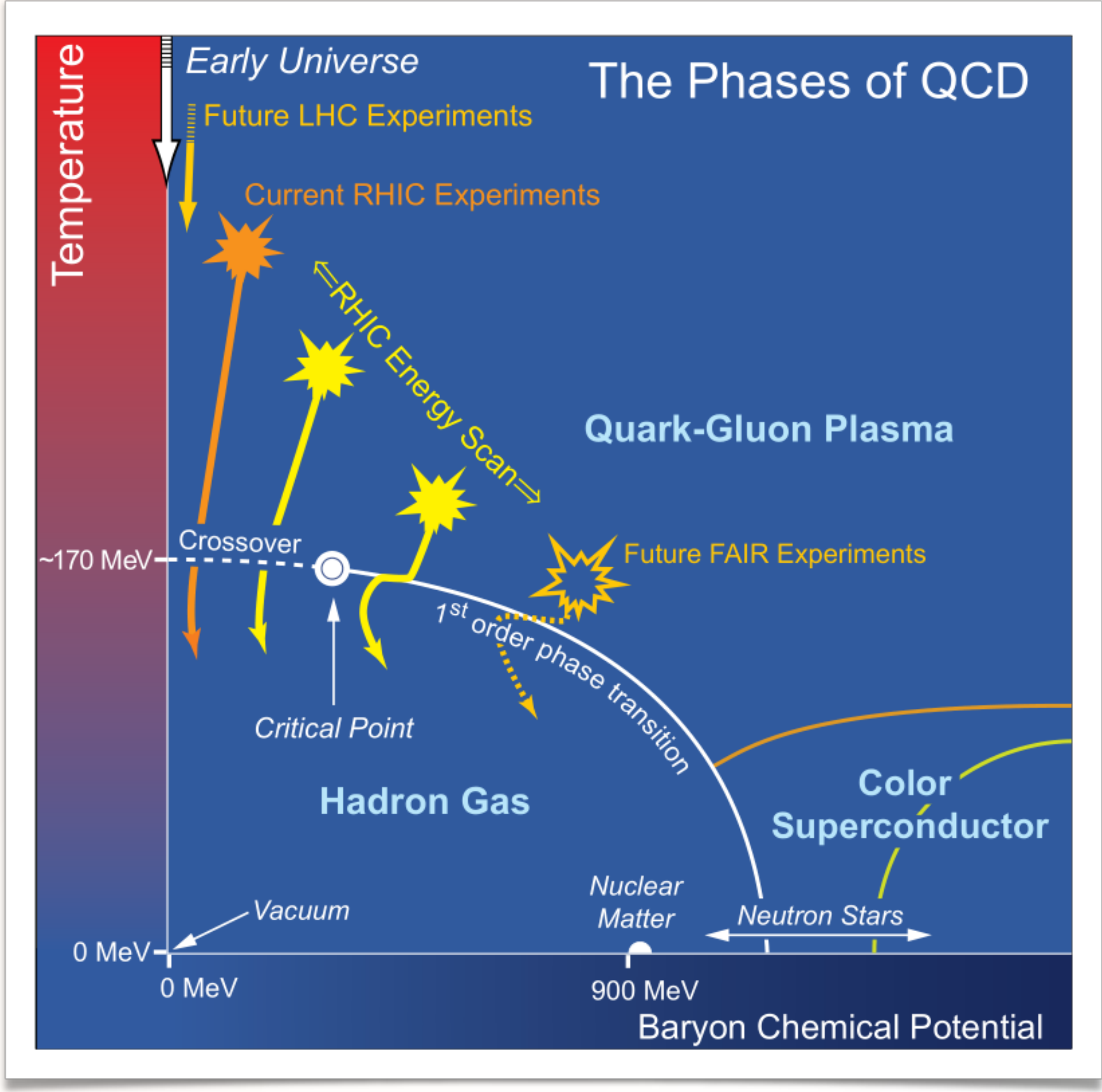

1. INTRODUCTION

• On experimental side, one could generate the matter at high temperature and low density even the warm dense matter with the relativistic heavy ion collisions (RHICs) in laboratory and study the corresponding phase transitions

• But for the phase transition at zero temperature and high density, we cannot rely on terrestrial experiment, and most data comes from the observation of compact stars.

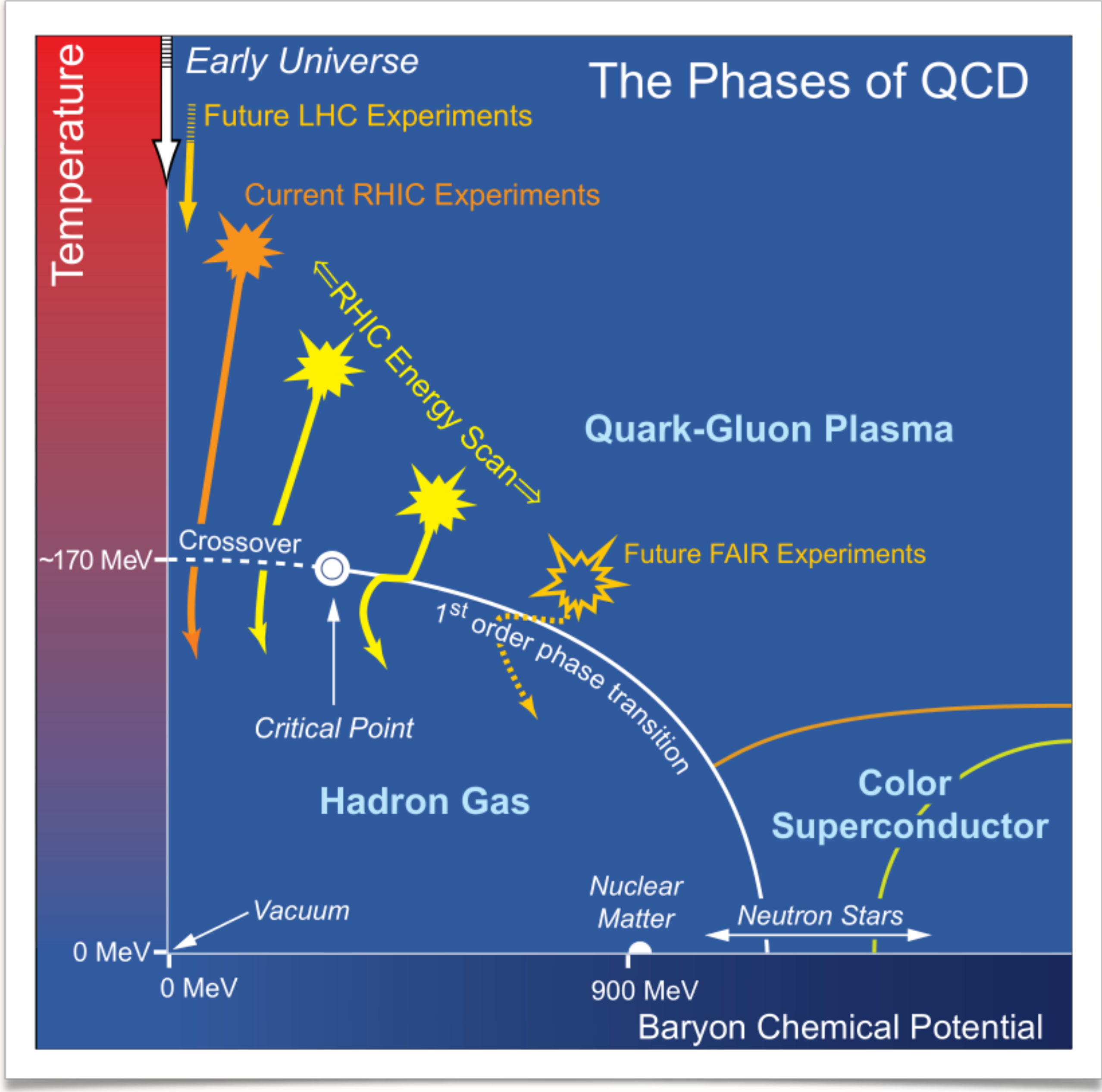

1. INTRODUCTION: Neutron Star Mass

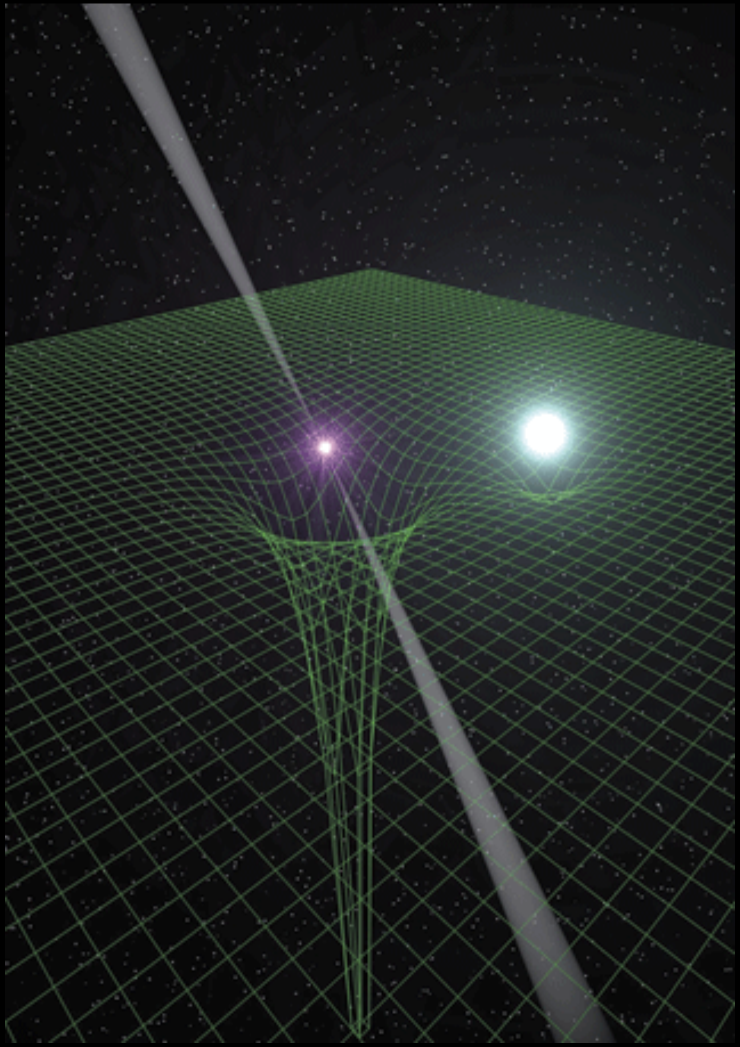

Artist's impression of the PSR J0348+0432 system.

- One of the most important quantity of neutron stars is their mass.

- Several years ago, two neutron stars with large mass were observed[1,2]. Therefore, the equation of states(EoS) of the neutron star matter must be stiff to support the star against its own gravity, which challenges our former theories.

- The possible appearance of hyperon greatly softens the EoS, and reduces the neutron star mass. This controversy is usually referred to as "hyperon puzzle".

[1] P. B. Demorest *et*. *al*., Nature (London) 467, 1081 (2010).
[2] J. Antoniadis et al., Science 340, 1233232 (2013).

1. INTRODUCTION: Tidal Deformability

- Another important observable is the gravitational wave.

- GW170817 is the first observation of gravitational wave of binary neutron star merger [1], and it marks a new era of multi-messenger astronomy.

- The tidal deformability of a $1.4M_{\odot}$ neutron star should be $\Lambda < 800$, which indicates that the EoS should be soft.

- Therefore, mass and tidal deformability together provide strong constraint on EoS.

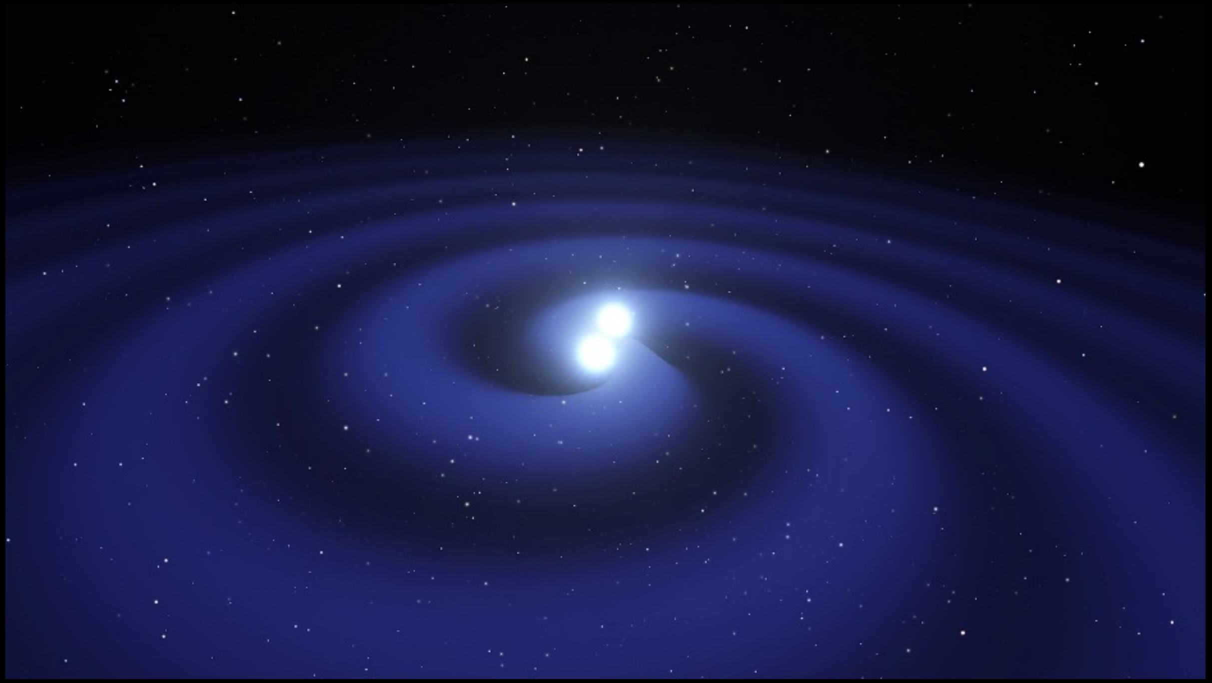

[1] B. P. Abbott et al., Astrophys. J. Lett. 848, L13 (2017).

1. INTRODUCTION

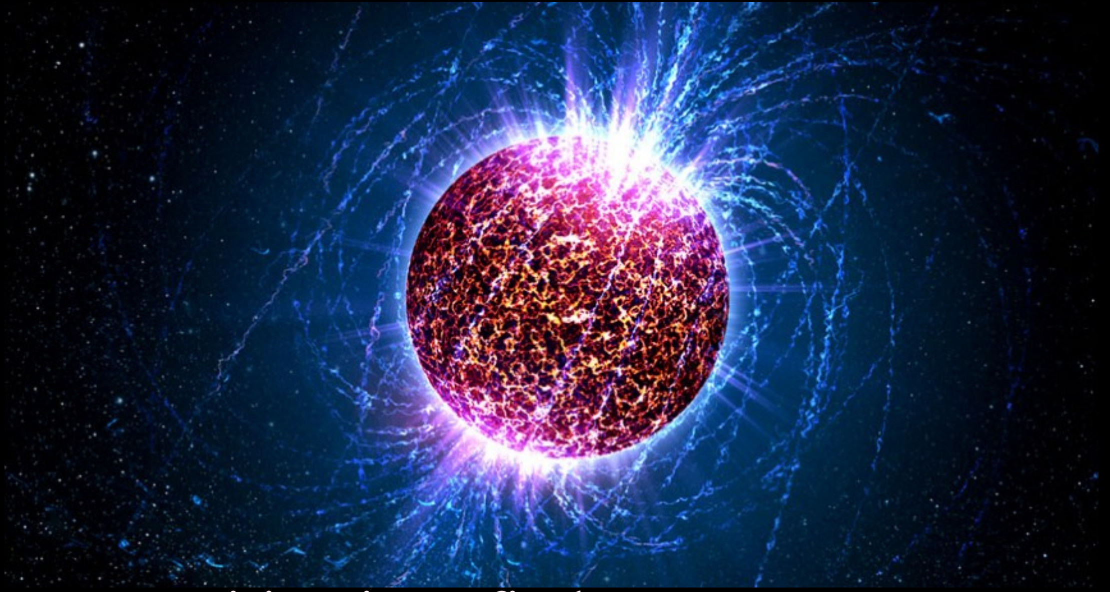

• On the theoretical side, lattice calculations fails at high chemical potential region, and we have to rely on models. Although the best way to study phase transition is to find a way to describe hadron matter and quark matter unitedly, but for cold dense astronuclear matter, we are now unable to find a very satisfying theory.

• The most common way to study hadron-quark phase transition is to describe hadron and quark matter separately with models, and use different construction schemes to combine them and get the equation of state for hybrid stars.

• Next we are going to introduce some construction schemes and the one we use in this work.

OUTLINE

1. **Introduction and Motivation**
2. **Constructing Hadron-Quark Phase Transition**

If we already know the way to describe hadron and quark matter separately, how to combine them to describe the phase transition? What will the hybrid star looks like?

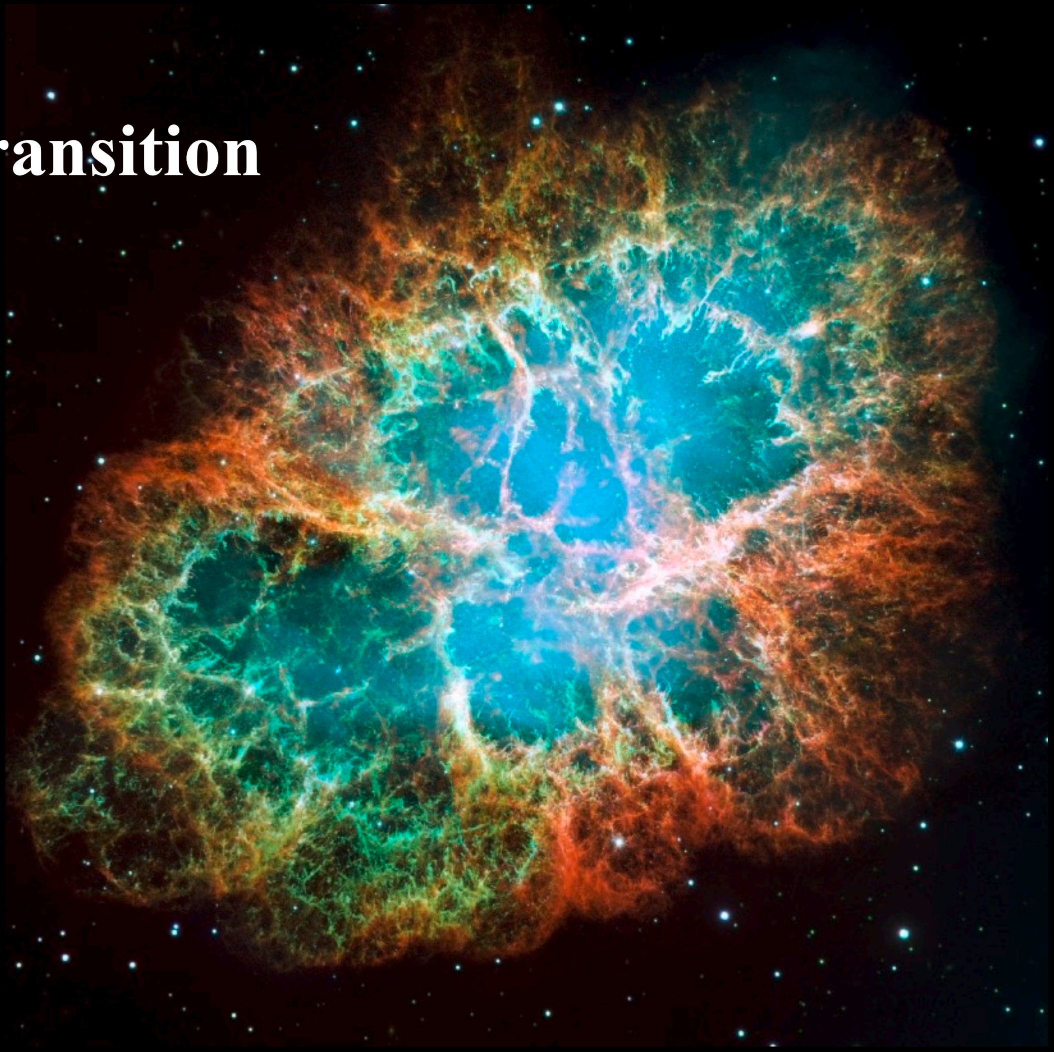

2. CONSTRUCTION:

RED: quark matter
BLUE: hadron matter

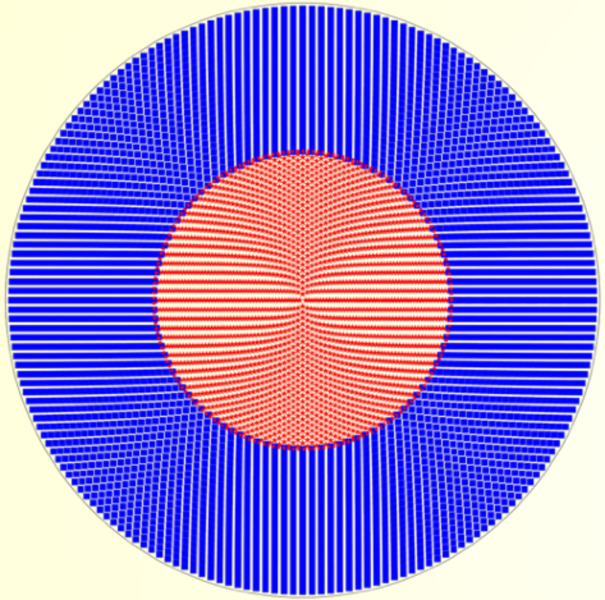

Maxwell

- Clear phase boundary.
- No mix phase.

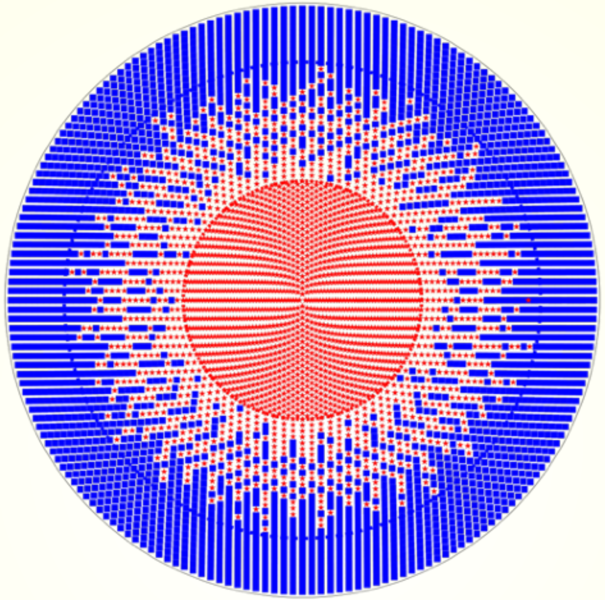

Gibbs

- Clear phase boundary.
- With mix phase.

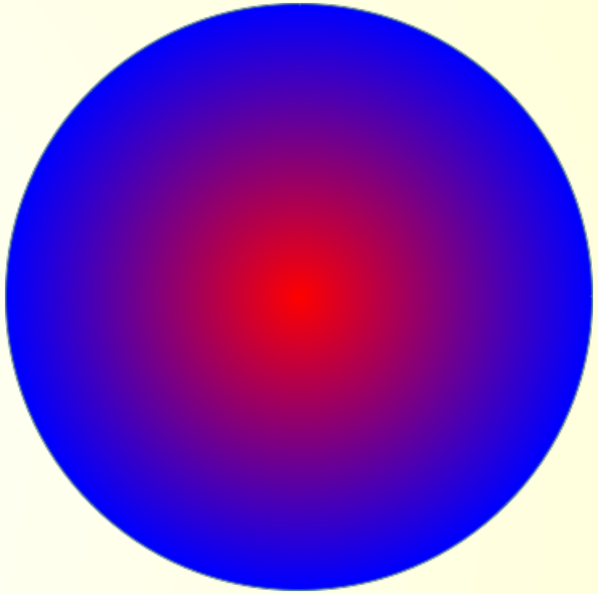

3-Window

- No clear phase boundary

2. CONSTRUCTION: Maxwell

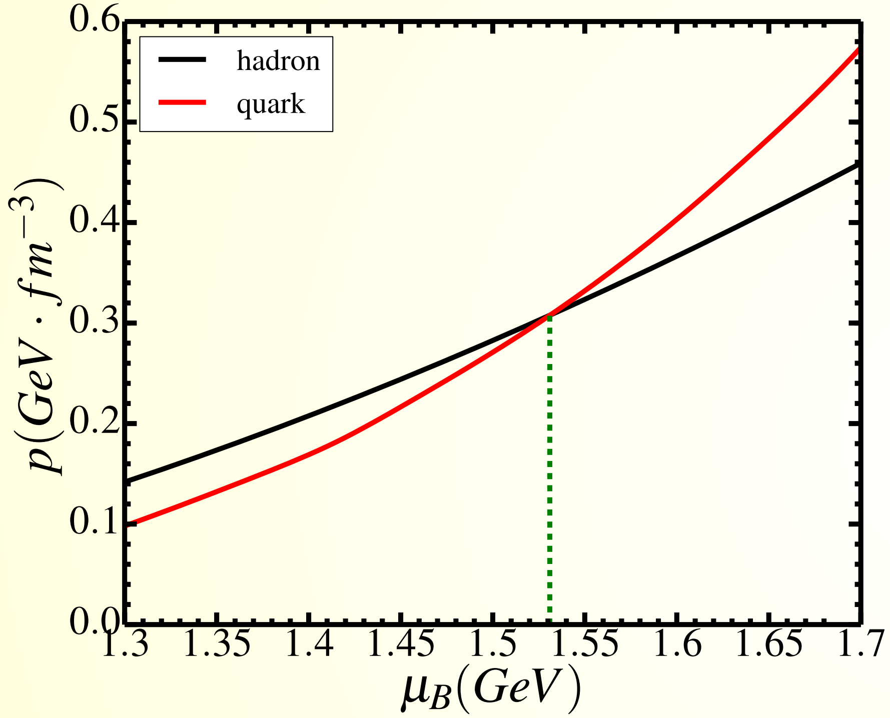

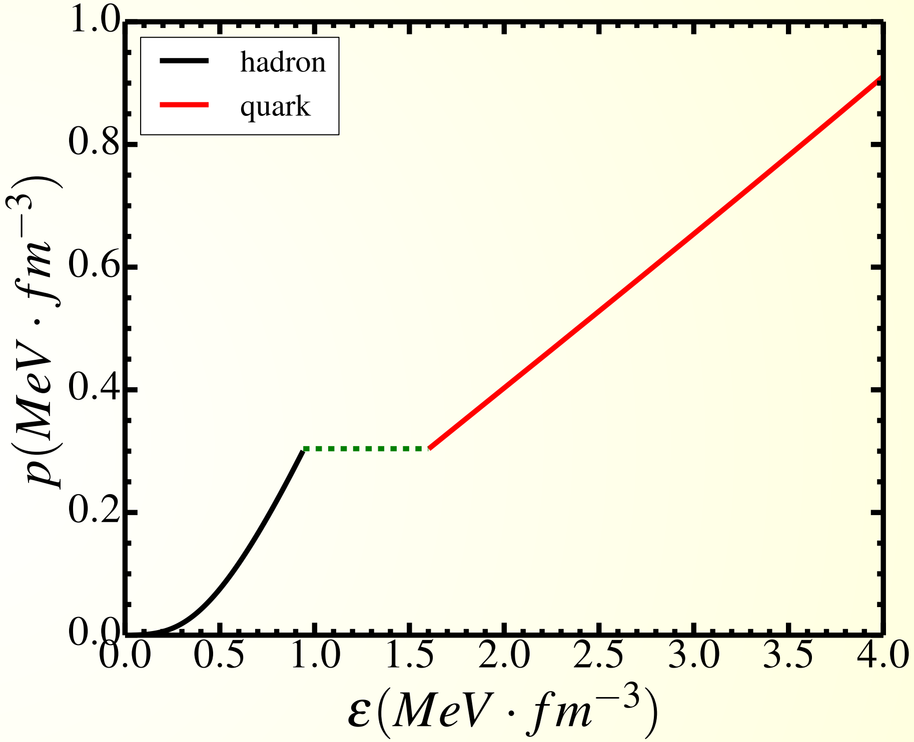

- Phase transition happens when p and μ_B in two phases are equal.
- The pressure remains constant in the phase transition region.
- We can calculate the speed of sound from EoS.

$$c_s^2 = \frac{\partial p}{\partial \varepsilon}$$

2. CONSTRUCTION: Maxwell

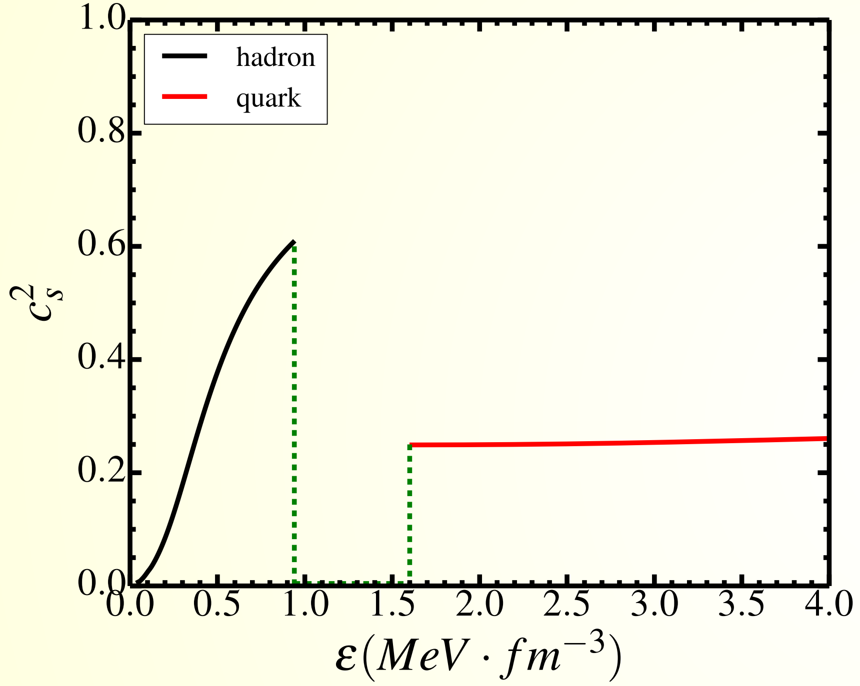

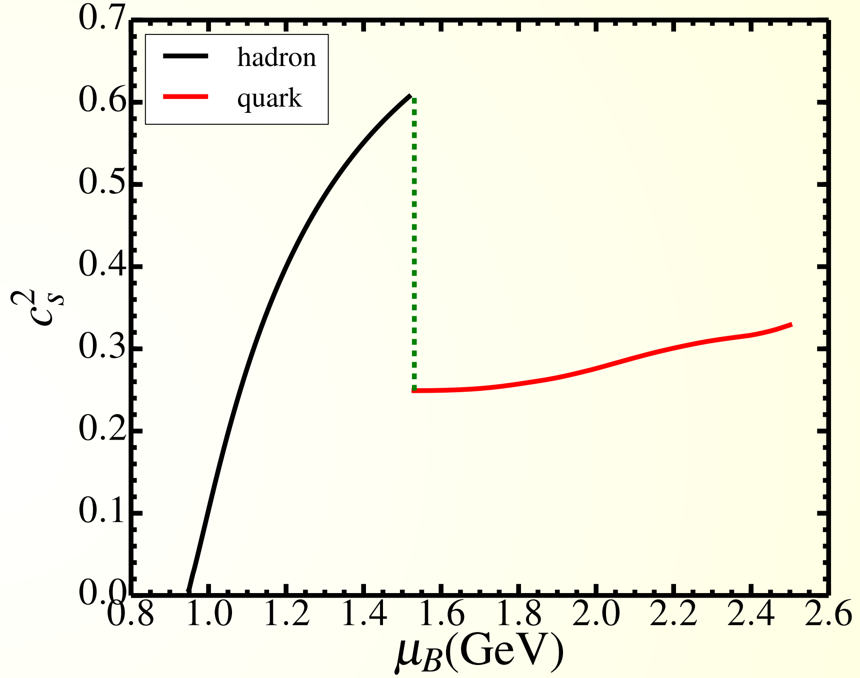

- The speed of sound vanishes in the phase transition region.
- On c_s^2-μ_B plane, there is a sudden jump at phase transition chemical potential.

$$c_s^2 = \frac{\partial p}{\partial \varepsilon}$$

2. CONSTRUCTION:

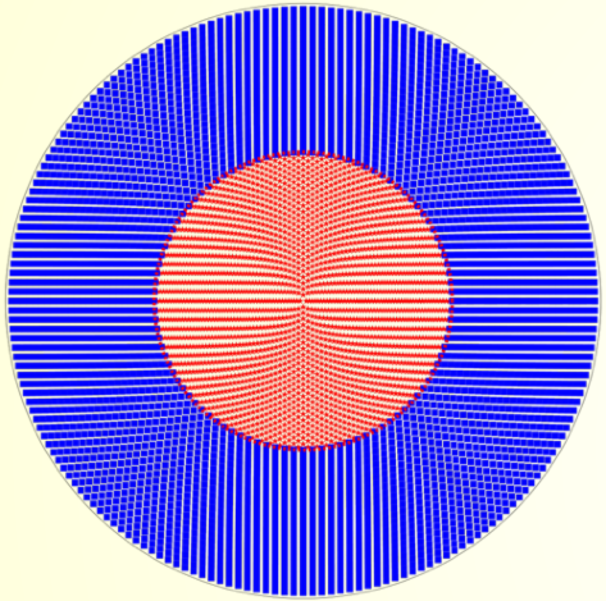

Maxwell

- There is a clear phase boundary.
- No mix phase.
- Infinite surface tension.
- Only one chemical potential.

● There are two conserved quantities:
baryon number and charge number.
And there should be two chemical potentials:
μ_B and μ_e.

2. CONSTRUCTION:

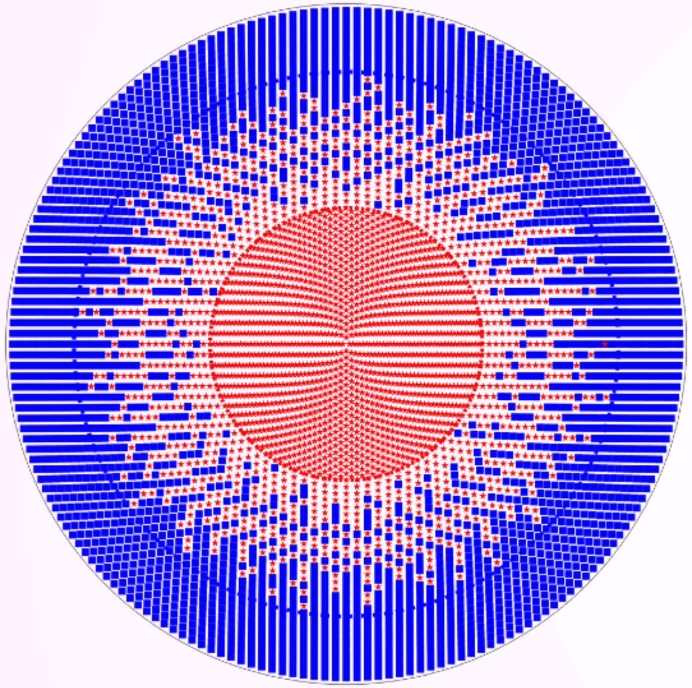

Gibbs

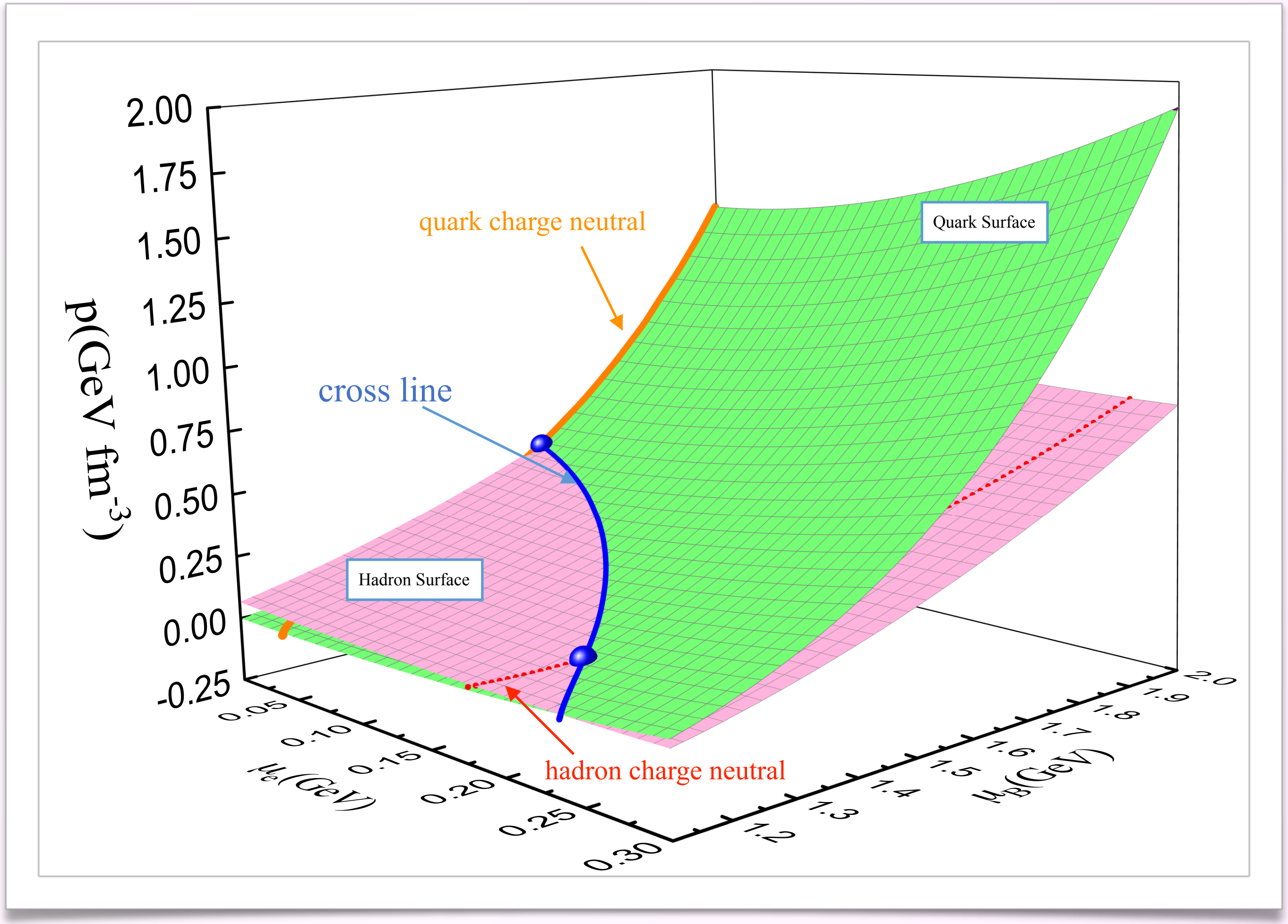

- Gibbs construction describe the phase transition with two chemical potentials

2. CONSTRUCTION: Gibbs

- $p(\mu_B,\mu_e)$ function corresponds to a surface.

- Applying charge neutral condition, the surface degenerates to a line.

- Phase transition occurs when p, μ_B and μ_e are equal in two phases.

- On the cross line, hadron and quark both charged as long as their charge cancel.

- The pressure changes first along the red line, then the blue line and finally the orange line.

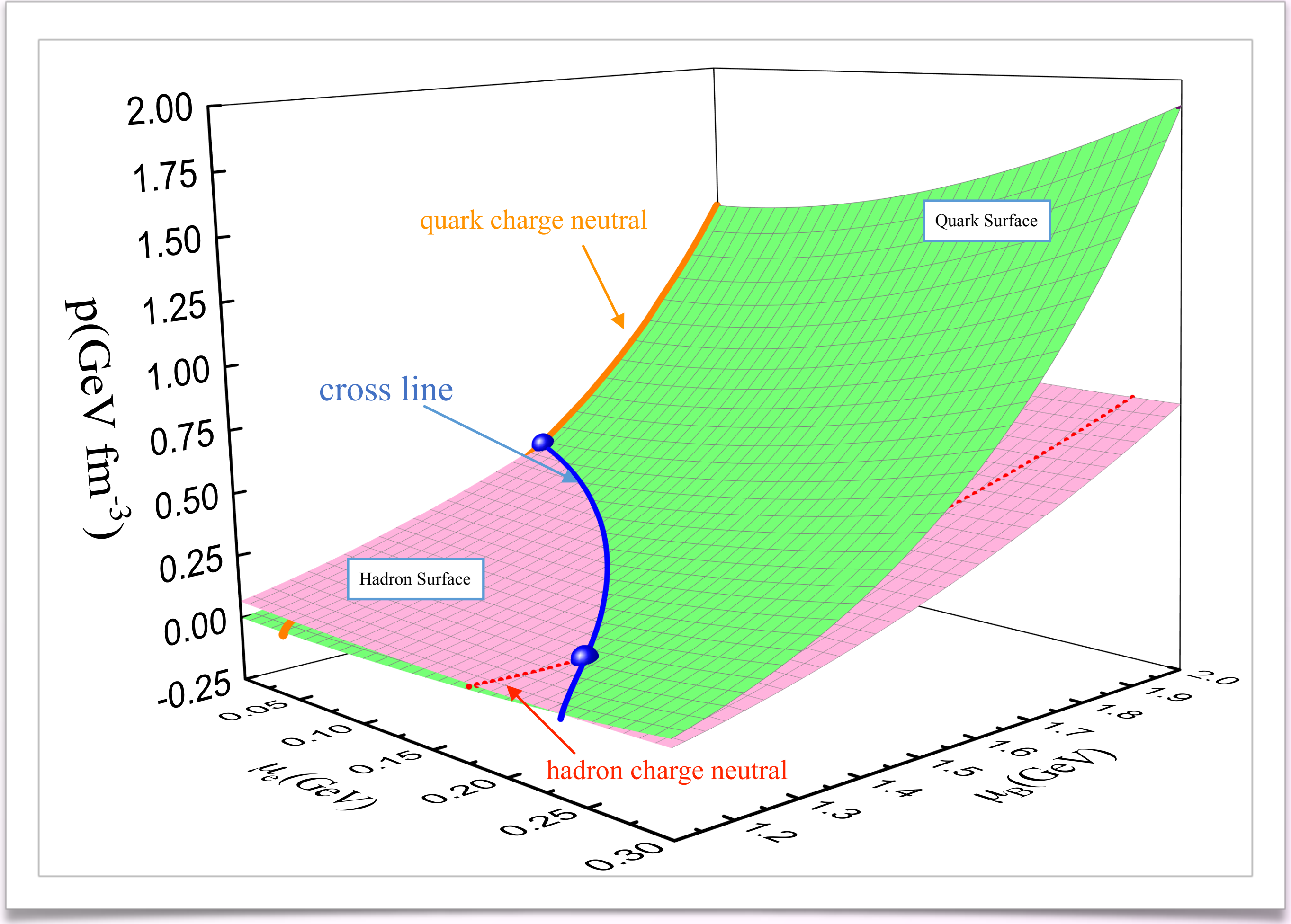

2. CONSTRUCTION: Gibbs

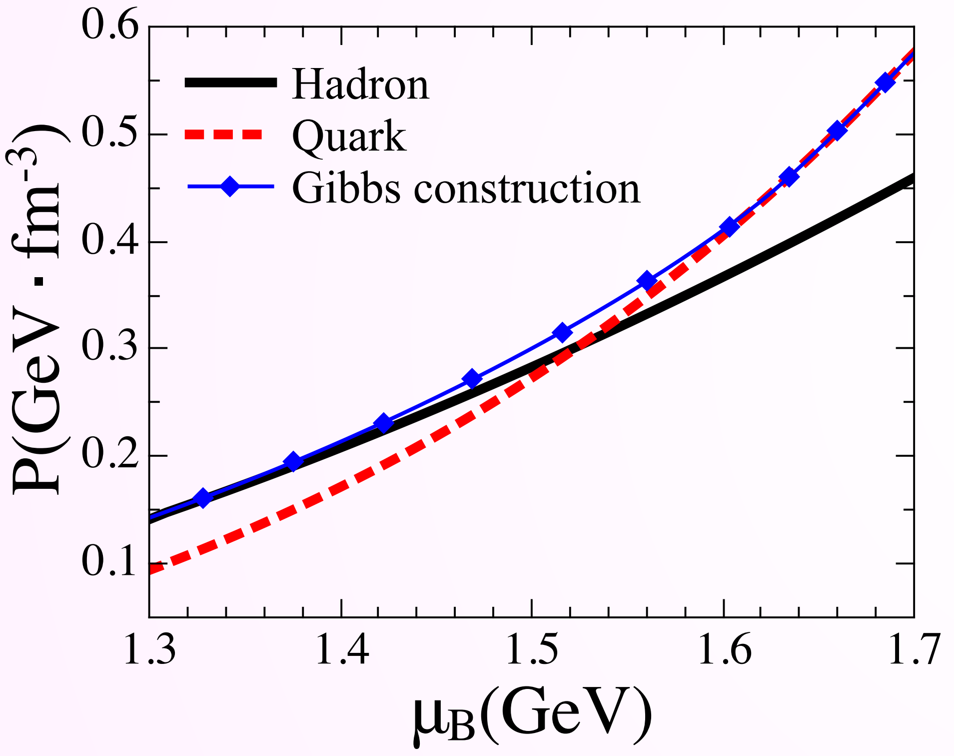

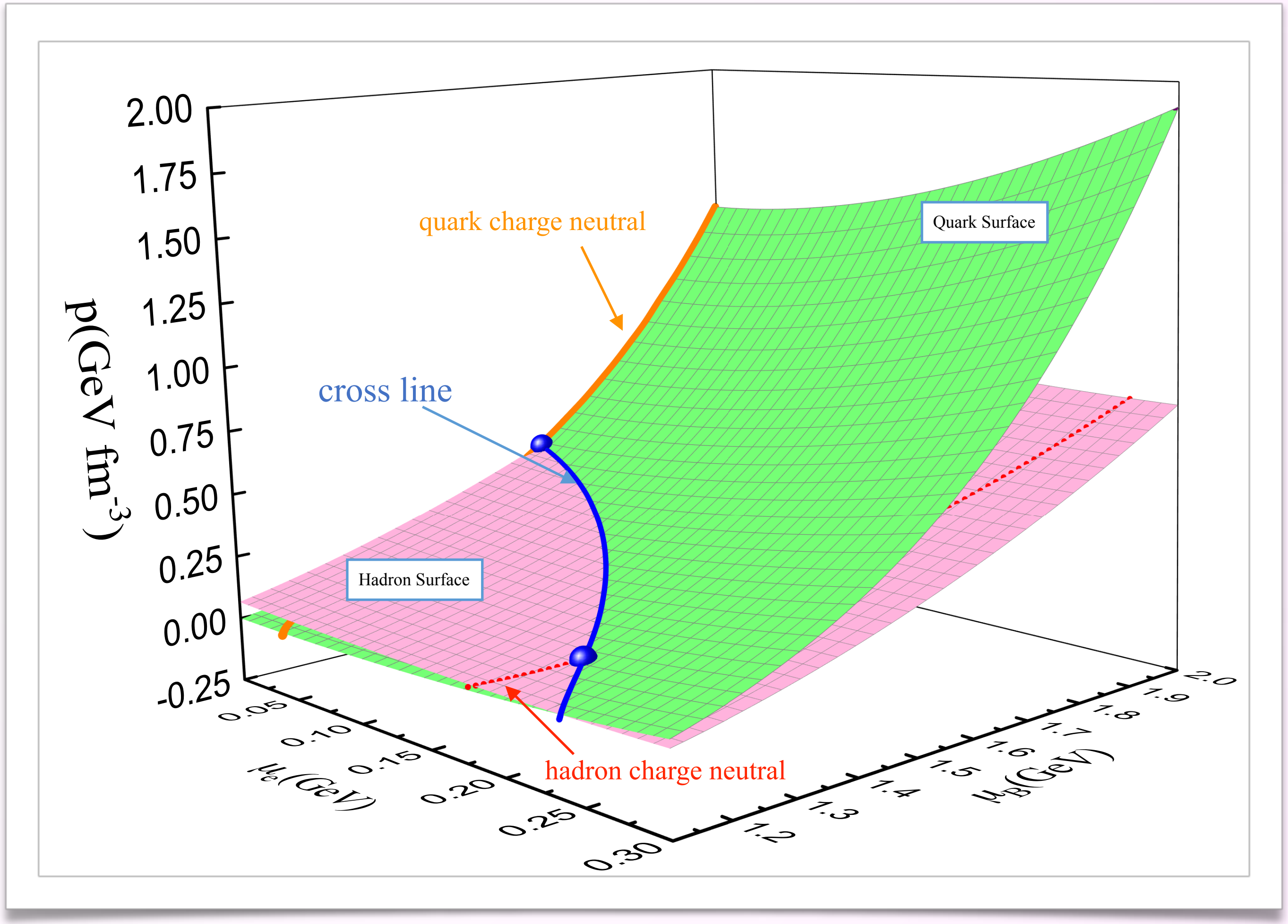

● The second derivative is not continuous at two conjunction points.

2. CONSTRUCTION: Gibbs

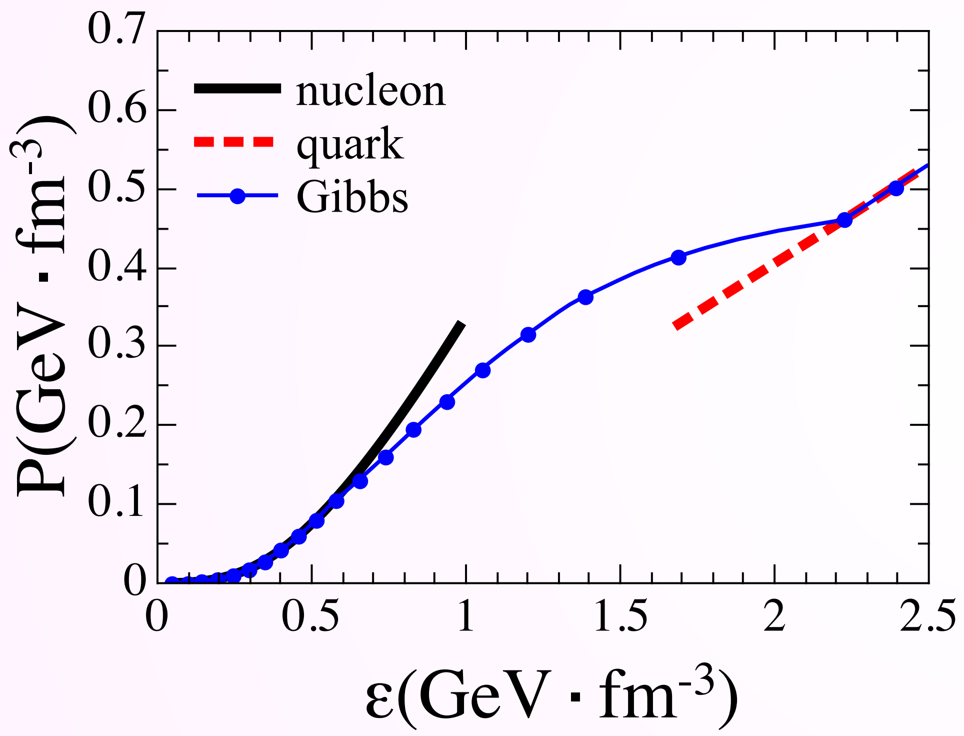

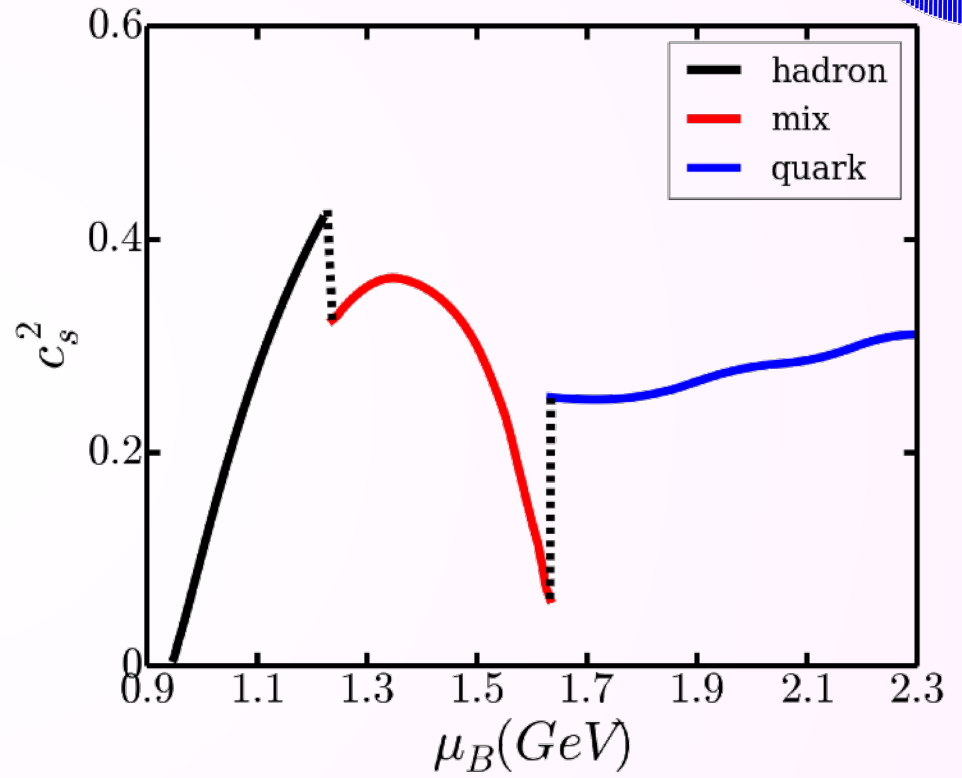

● At the beginning and ending of the phase transition, the EoS is not smooth, and the speed of sound is not continuous.

2. CONSTRUCTION:

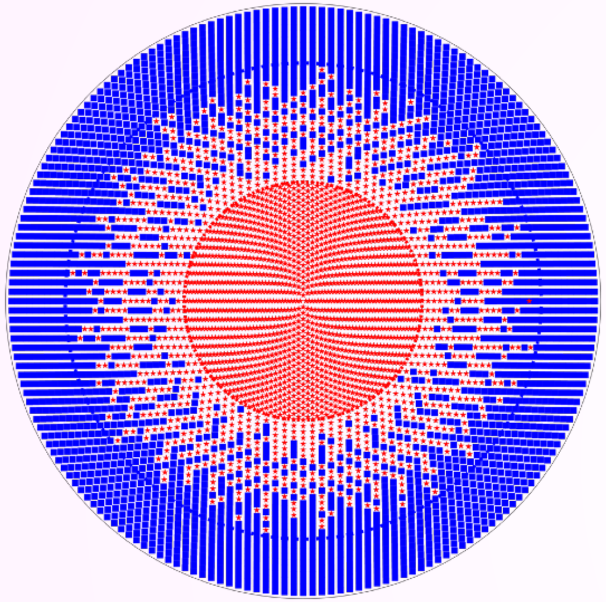

Gibbs

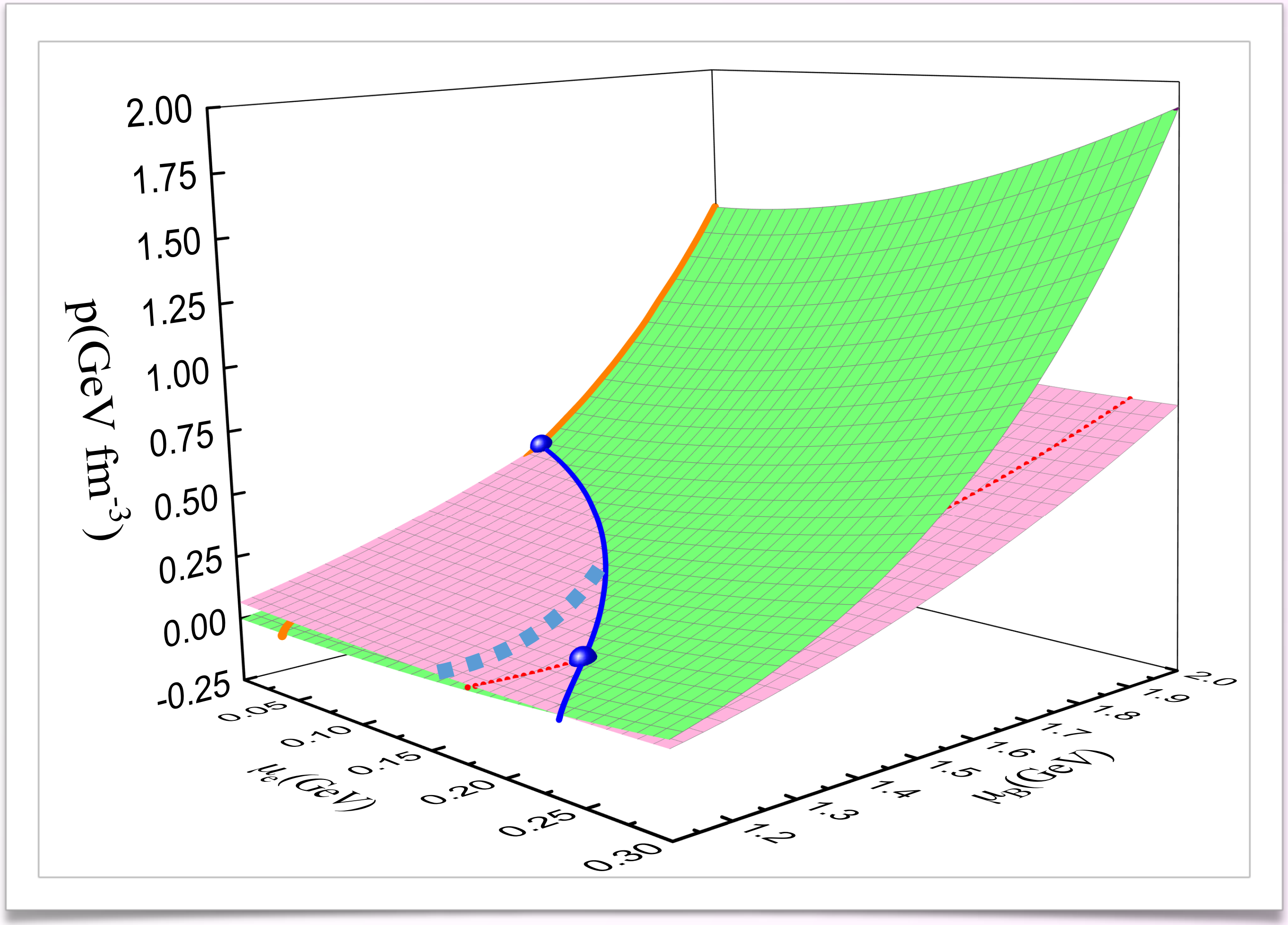

- There is a region where hadron and quark matter coexist.
- Hadron and quark models are inaccurate at phase transition region.
- The phase transition may even not happen under Gibbs construction.
- In order to avoid this problem, 3-window construction was proposed.

2. CONSTRUCTION: 3-Window

- Use interpolation to get EoS at phase transition region.
- Interpolating energy density with wight function[1]

$$\varepsilon(\rho) = \varepsilon_H(\rho) f_-(\rho) + \varepsilon_Q(\rho) f_+(\rho)$$

- Interpolating pressure with polynomial function[2]

$$p_{\mathrm{middle}}(\mu) = \sum_{m=0}^{N} b_m \mu^m$$

- Interpolating pressure with piecewise polynomial[3]

$$p_i(\rho) = \kappa_i \rho^{\gamma^i}, \ \mu \in [\mu_{i-1}, \mu_i]$$

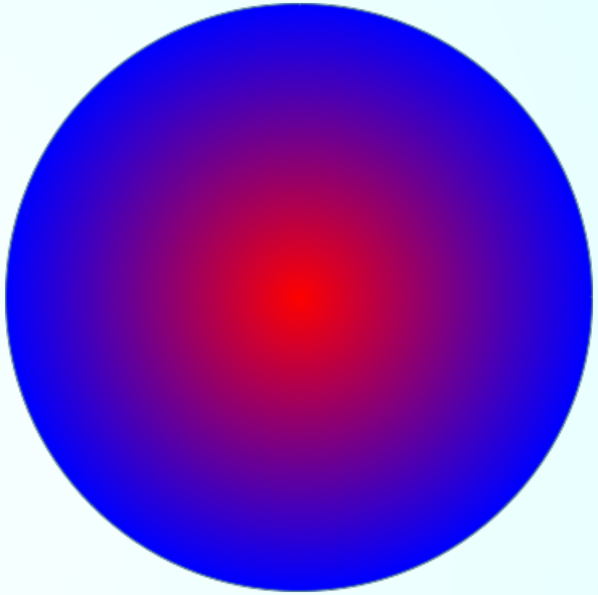

[1]K. Masuda et al, arXiv:1212.6803
[2]T. Kojo et al, arXiv:1412.1108
[3]E. Annala et al, arXiv:1711.02644

- Not explicitly include first order hadron-quark phase transition.

2. CONSTRUCTION: 3-Window

- The 3-window construction claim that the hadron-quark phase transition in neutron stars should be a cross-over.
- But Dyson-Schwinger calculations suggest that it should be first-order.

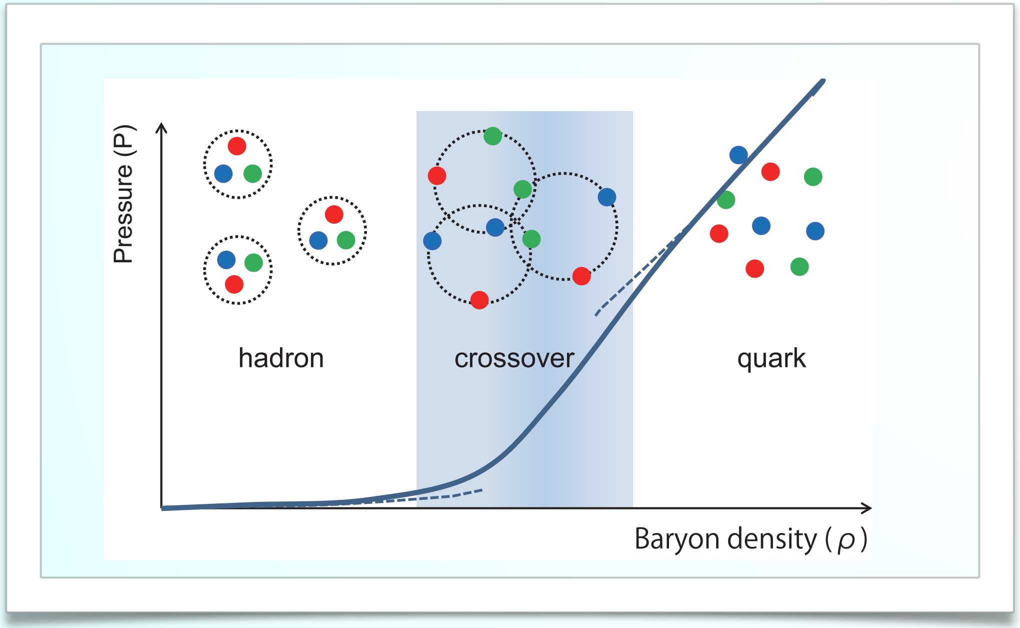

A schematic figure of a crossover phase transition.
Taken from K. Masuda et al, arXiv:1212.6803.

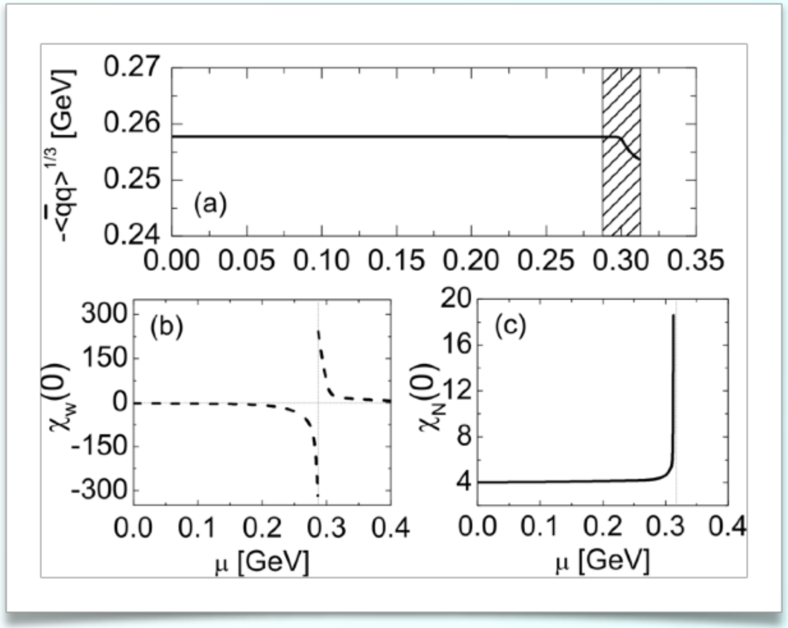

Dyson-Schwinger calculations of chiral condensate and chiral susceptibility.
Taken from S. X. Qin, et. al.,
Phys. Rev. Lett. 106, 172301 (2011);

2. CONSTRUCTION:

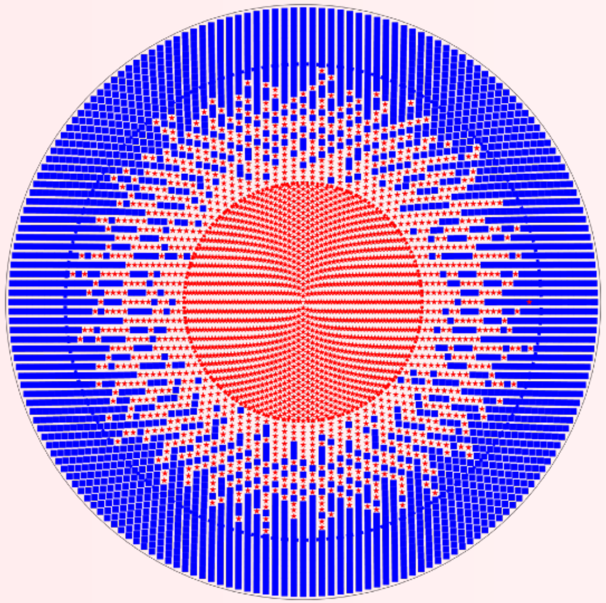

+

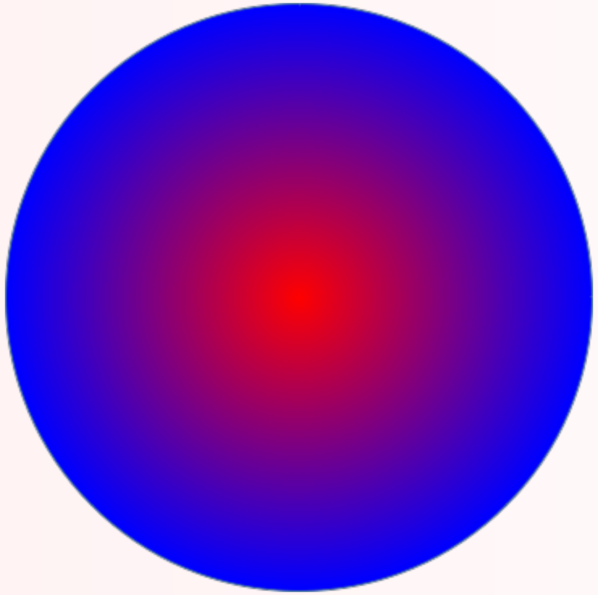

= ?

Gibbs

First-order phase transition

3-Window

Avoiding inaccuracy

2. CONSTRUCTION: Sound Speed Interpolation

- The sound speed is not continuous when phase transition happens
- We parameterize sound speed to interpolate the EoS.
- We use a quadratic function to describe sound speed in phase transition region.
- There are five parameters for the construction: A, B and C for the quadratic function, and two chemical potentials describing the phase transition region.

$$c_s^2 = \frac{\partial p}{\partial \varepsilon} \Rightarrow \frac{\partial n_B}{\partial \mu_B} = \frac{n_B}{\mu_B c_s^2(\mu_B)}$$

$$\frac{\partial p}{\partial \mu_B} = n_B$$

Boundary Condition:

$$n(\mu_0) = n_H(\mu_0)$$

$$p(\mu_0) = p_H(\mu_0)$$

$$c_s^2(\mu_B) = A\mu_B^2 + B\mu_B + C$$

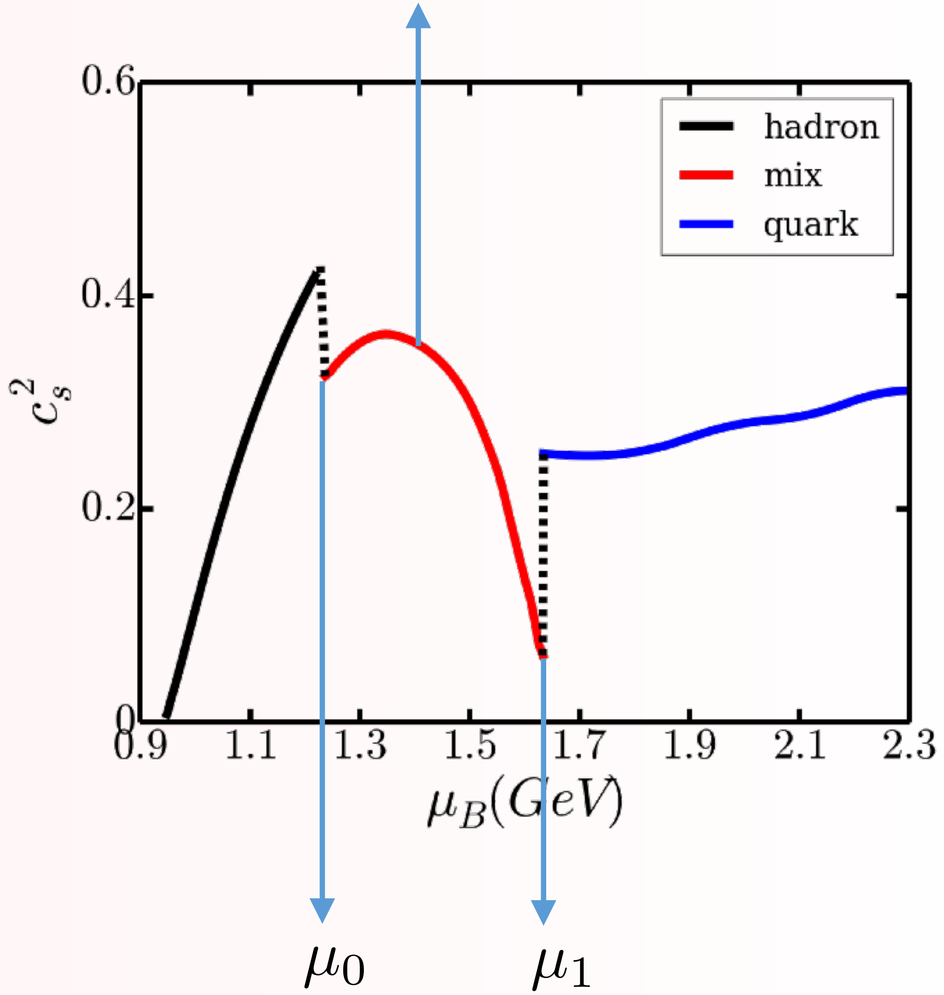

2. CONSTRUCTION: Sound Speed Interpolation

● The solution of differential equation may not approach quark EoS at high density. We must introduce additional constraints:

$$p(\mu_1) = p_Q(\mu_1)$$
$$n(\mu_1) = n_Q(\mu_1)$$

● We can use these two constraints to fix two of the A,B and C parameter from quadratic function, and there are three free parameters left for the construction scheme.

● In practice, we choose the following three parameters: the chemical potential corresponding to the starting and ending of the phase transition, and the sound speed at the center of the phase transition region.

$$c_s^2(\mu_B) = A\mu_B^2 + B\mu_B + C$$

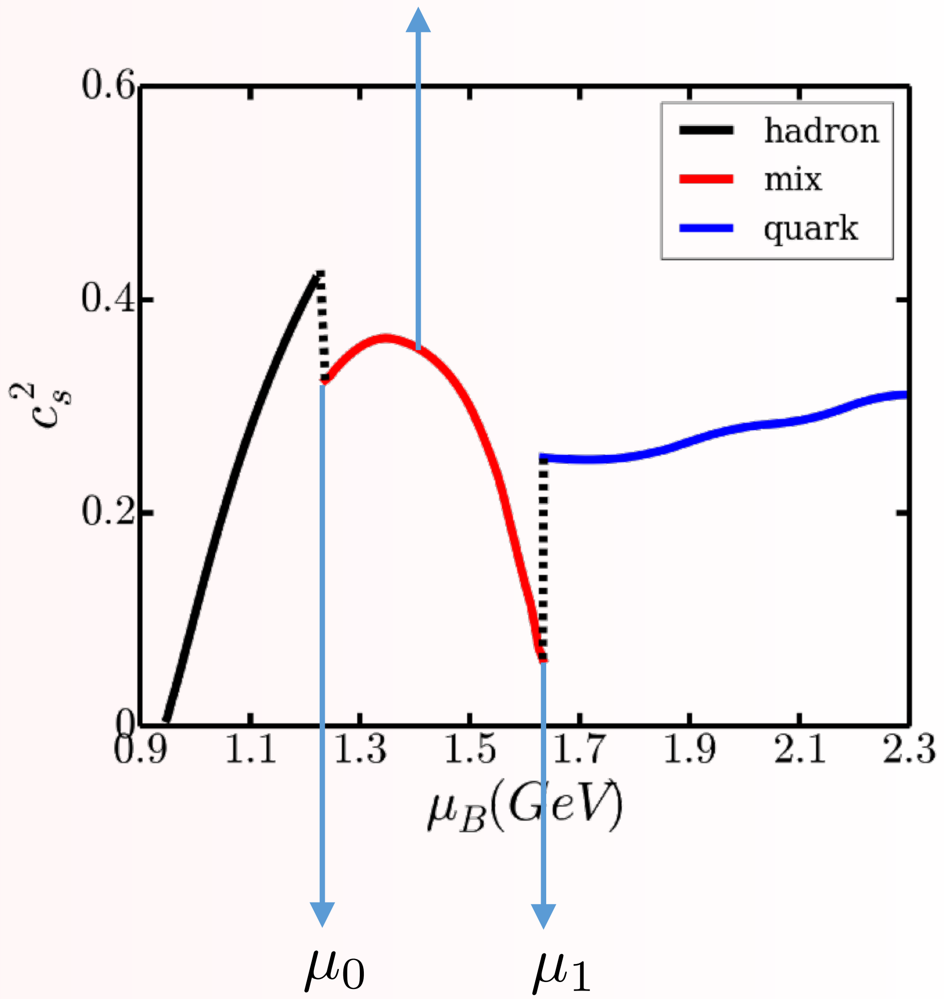

OUTLINE

1. Introduction and Motivation
2. Constructing Hadron-Quark Phase Transition
3. Hadron Model and Quark Model

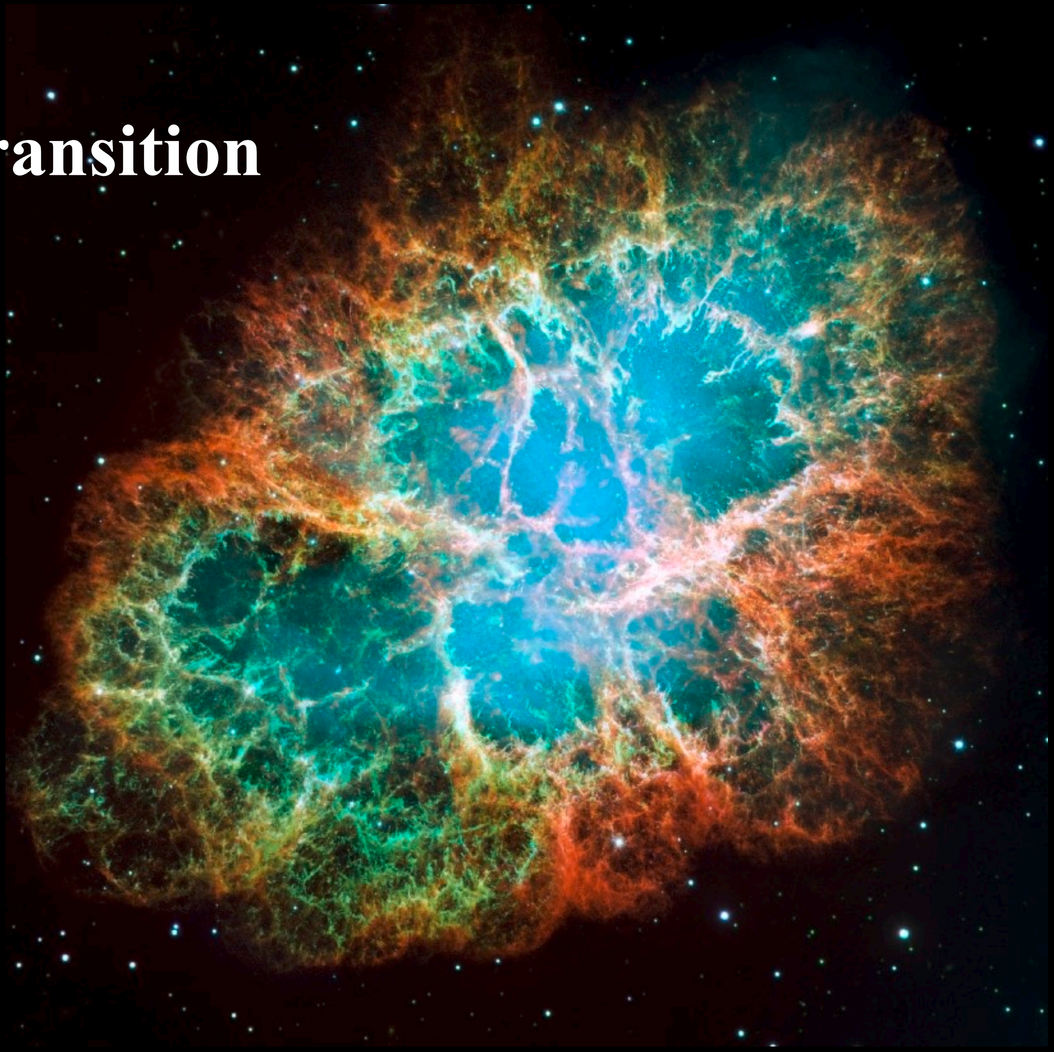

Hadron Model: Relativistic Mean Field Theory[1]

$$\mathcal{L} = \sum_N \bar{\Psi}_N \Big[i\gamma_\mu \partial^\mu - (m_N - g_\sigma \sigma) - g_\omega \gamma_\mu \omega^\mu - g_\rho \gamma^\mu \vec{t}_N \cdot \vec{\rho}_\mu \Big] \Psi_N$$
$$+\frac{1}{2}\left(\partial_\mu \sigma \partial^\mu \sigma - m_\sigma^2 \sigma^2\right) + \frac{1}{2} m_\omega^2 \omega_\mu \omega^\mu - \frac{1}{4}\omega_{\mu\nu}\omega^{\mu\nu} + \frac{1}{2} m_\rho^2 \vec{\rho}_\mu \cdot \vec{\rho}^\mu - \frac{1}{4}\vec{\rho}_{\mu\nu} \cdot \vec{\rho}^{\mu\nu}$$
$$+\sum_l \bar{\Psi}_l \left(i\gamma_\mu \partial^\mu - m_l\right)\Psi_l$$

1) Under mean field approximation, the system is assumed to be in a static and uniform ground state. The partial derivative of the meson field disappear.

2) Use Euler-Lagrange equation to get field equation. $\partial_\mu \frac{\partial \mathcal{L}}{\partial(\partial_\mu \phi)} - \frac{\partial \mathcal{L}}{\partial \phi} = 0$

3) The equation of state can be calculated from lagrangian.

$$\mathcal{T}^{\mu\nu} \equiv \frac{\partial \mathcal{L}}{\partial(\partial_\mu \psi_i)} \partial^\nu \psi_i - \eta^{\mu\nu} \mathcal{L} \qquad \epsilon = \langle \mathcal{T}^{00} \rangle \qquad p = \frac{1}{3}\langle \mathcal{T}^{ii} \rangle$$

[1] S. Typel and H. H. Wolter, Nucl. Phys. A, 656, 331-364 (1999)

Quark Model: Dyson-Schwinger Equation[1]

[1]H. Chen et al, Phys. Rev. D, 84, 105023(2013)

DSE for quarks

Gluon: $$\frac{\mathcal{G}(k^2;\mu)}{k^2} = \frac{4\pi^2 D}{\omega^6} k^2 e^{-\alpha\mu^2/\omega^2} e^{-k^2/\omega^2}$$

$$S(p;\mu)^{-1} = Z_2\left[i\vec{\gamma}\cdot\vec{p} + i\gamma_4(p_4 + i\mu) + m_q\right] + \Sigma(p;\mu)$$

$$\Sigma(p;\mu) = Z_1 \int \frac{d^4q}{(2\pi)^4} g^2 D_{\rho\sigma}(p-q;\mu)\frac{\lambda^a}{2}\gamma_\rho \times S(q;\mu)\Gamma^a_\sigma(q,p;\mu)$$

Assumption for interaction

$$\Gamma_\sigma(q,p) = \gamma_\sigma$$

Quark Model: Dyson-Schwinger Equation[1]

equation of state

[1]H. Chen et al, Phys. Rev. D, 84, 105023(2013)

$$p = p(\varepsilon)$$

$$p = p(\mu)$$

$$n_q = n_q(\mu)$$

$$f_q(|\vec{p}|;\mu)$$

DSE for quarks

Gluon: $\frac{\mathcal{G}(k^2;\mu)}{k^2} = \frac{4\pi^2 D}{\omega^6} k^2 e^{-\alpha\mu^2/\omega^2} e^{-k^2/\omega^2}$

$$S(p;\mu)^{-1} = Z_2\left[i\vec{\gamma}\cdot\vec{p} + i\gamma_4(p_4 + i\mu) + m_q\right] + \Sigma(p;\mu)$$

$$\Sigma(p;\mu) = Z_1 \int \frac{d^4q}{(2\pi)^4} g^2 D_{\rho\sigma}(p-q;\mu)\frac{\lambda^a}{2}\gamma_\rho \times S(q;\mu)\Gamma^a_\sigma(q,p;\mu)$$

Assumption for interaction

$$\Gamma_\sigma(q,p) = \gamma_\sigma$$

DSE for quarks

$$f_q(|\vec{p}|;\mu) = \frac{1}{4\pi}\int dp_4 \mathrm{tr_D}\left[-\gamma_4 S_q(p;\mu)\right]$$

OUTLINE

1. Introduction and Motivation
2. Constructing Hadron-Quark Phase Transition
3. Hadron Model and Quark Model
4. Numerical Results

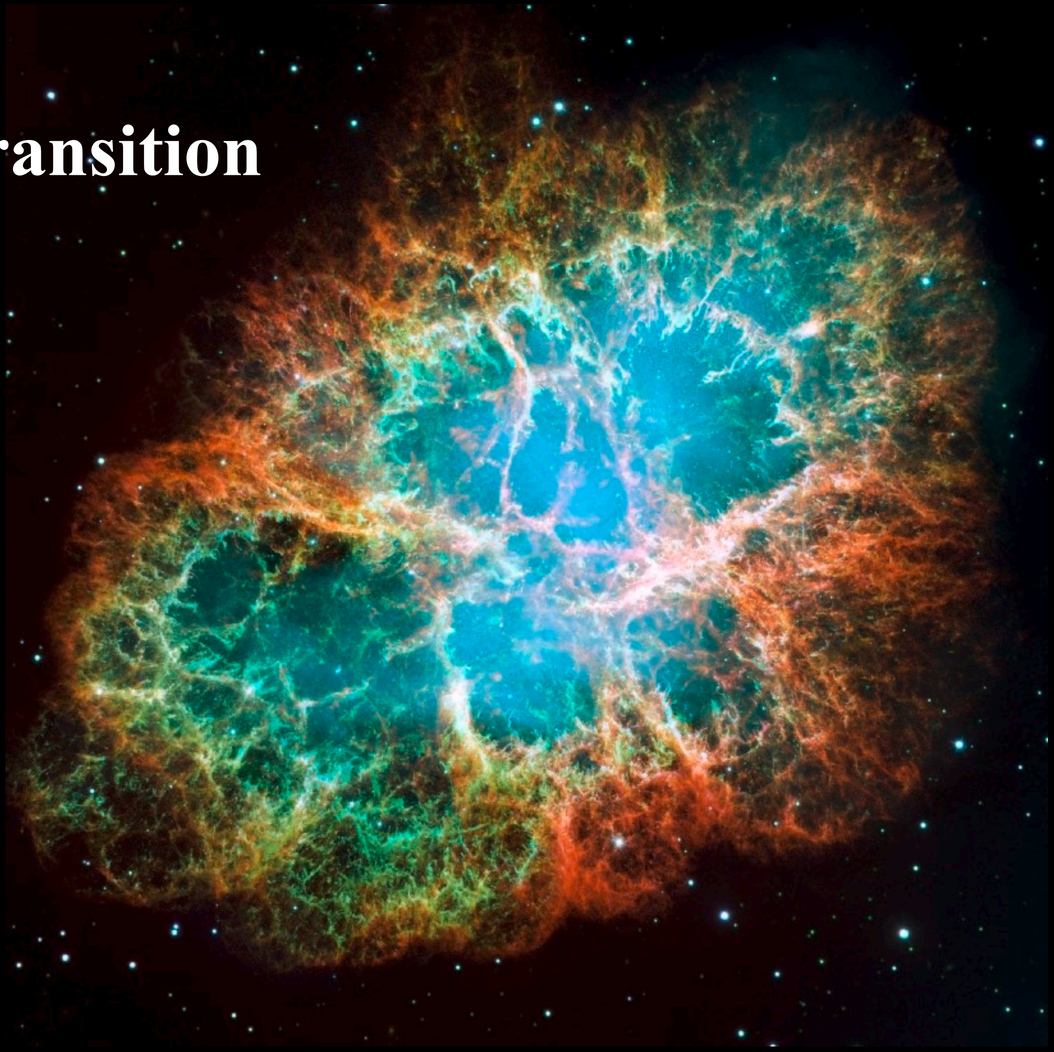

4. Numerical Results

- We use RMF for hadron, DSE for quark, and sound speed construction for phase transition.
- Using different parameters, we construct about 200000 EoS. All the parameters are uniformly distributed in their range.

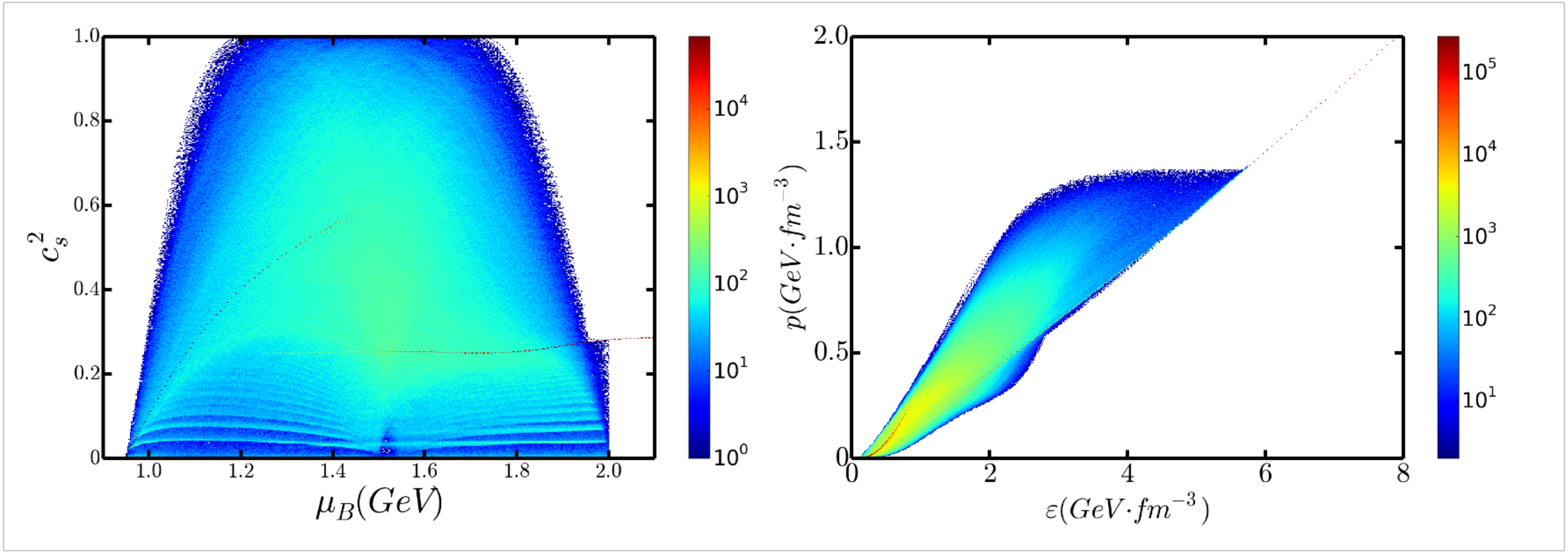

4. Numerical Results: Mass-Radius

● For every EoS, we can calculate the mass-radius relation and the tidal deformability from general relativity.

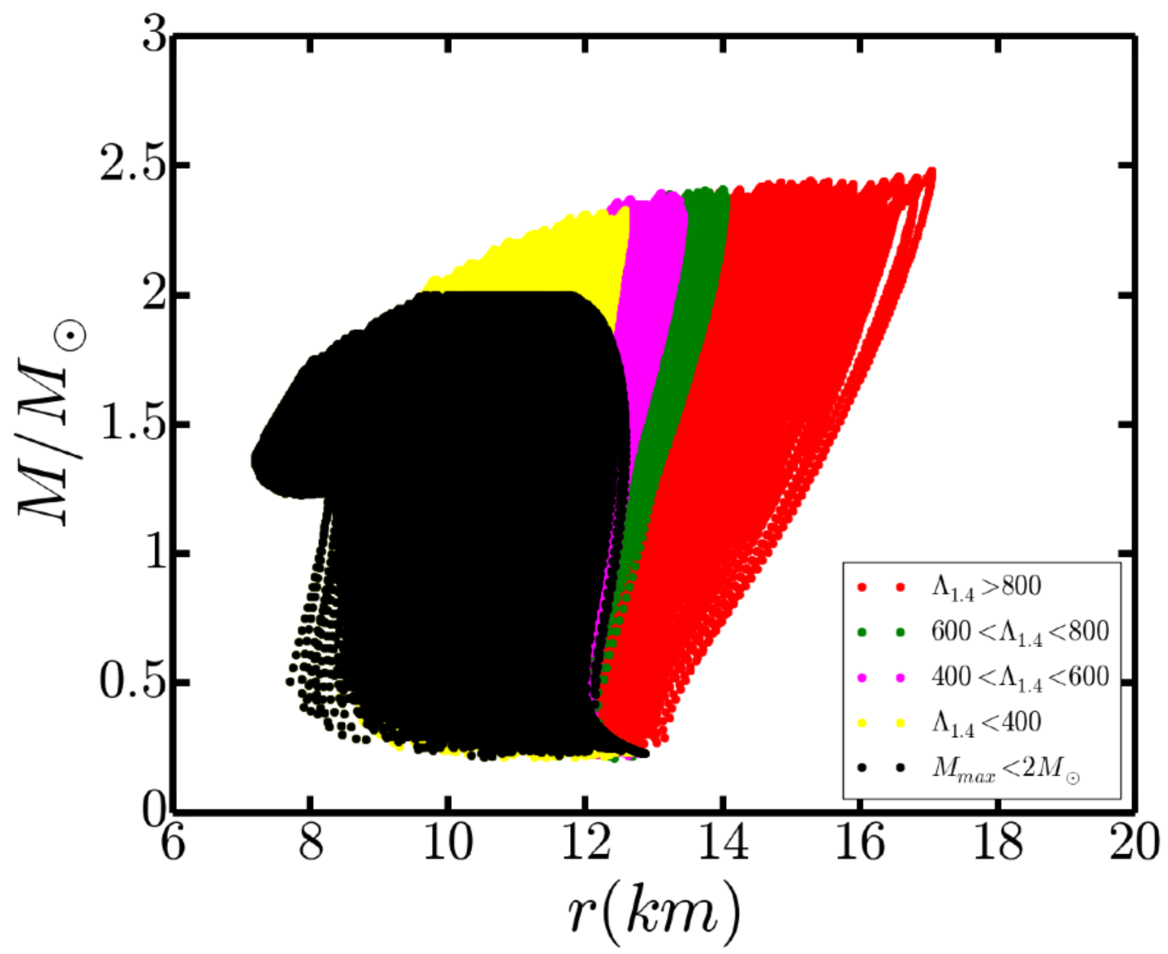

The Maximum mass of our construction is:

$$M_{\max} \leq 2.48 M_\odot$$

For a 1.4-solar-mass hybrid star, the range of radius and tidal deformability are:

$$8.18 \leq R_{1.4} \leq 15.50$$

$$14.83 \leq \Lambda_{1.4} \leq 2558.11$$

4. Numerical Results

[1]B. Margalit and B. Metzger, Astrophys. J. 850, L19 (2017)
[2]E. Annala et al, Phys. Rev. Lett., 120, 172703 (2018)

- We use the following constraints to exclude most of the constructed sound speed and EoS .

$$2 < \frac{M_{\max}}{M_{\odot}} < 2.16 \quad [1] \qquad 120 < \Lambda_{1.4} < 800 \quad [2] \qquad 9.9 < R_{1.4} < 13.6 \quad [2]$$

- The remaining sound speed and EoS are plotted as follow.

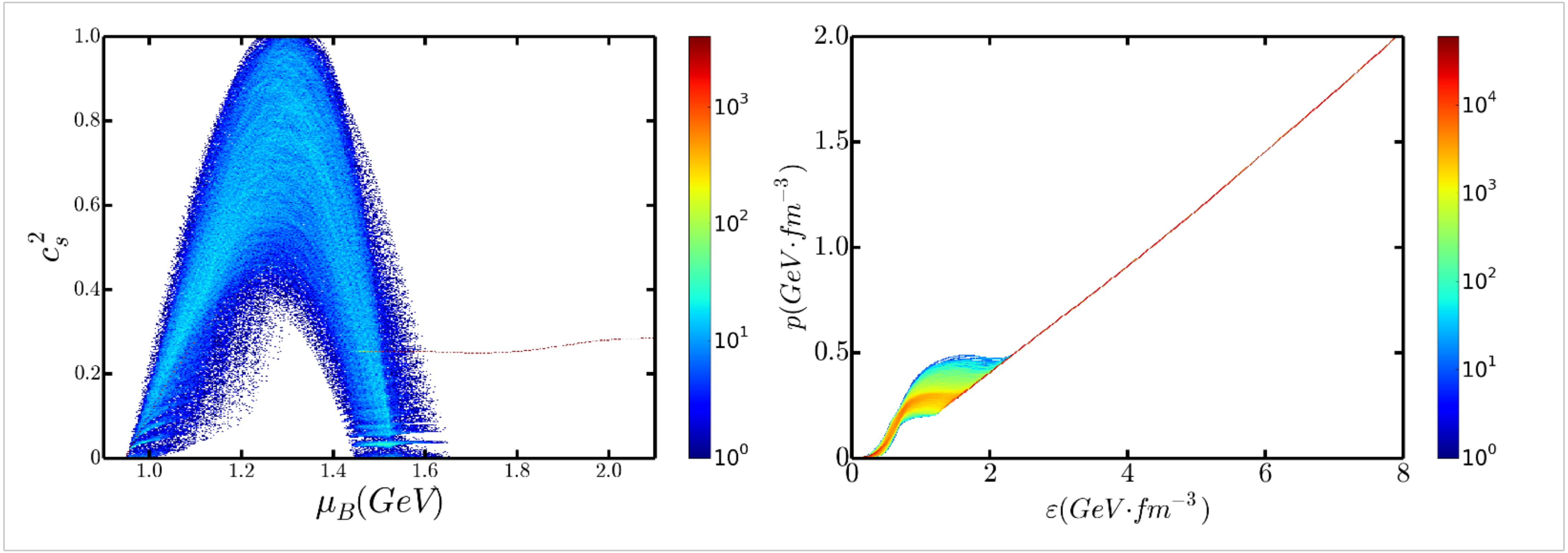

4. Numerical Results: PT chemical potential

● Next, we see how the astronomical observation can restrict our parameters.

● In this figure we plot the number of EoS with μ_0 taking different values, where μ_0 is the chemical potential corresponding to the starting of phase transition.

● The constraints on tidal deformability and radius do not change the range of μ_0

● An lower boundary of maximum mass sets the upper limit of μ_0

● The lower limit of μ_0 cannot be determined by astronomical quantities.

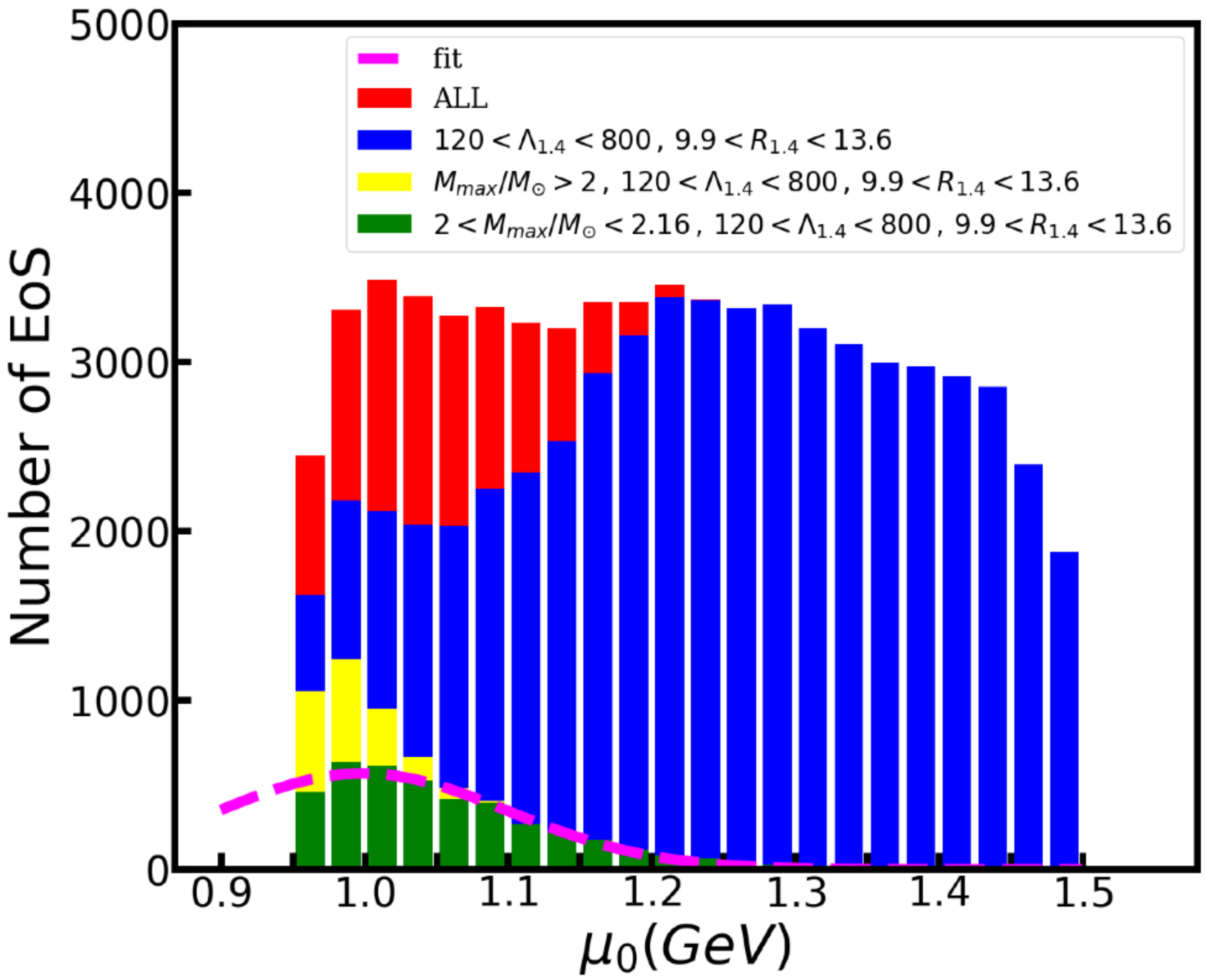

4. Numerical Results: PT chemical potential

- The upper limit of μ_0 is 1.32 GeV, which corresponds to a baryon number density of $4.11n_s$, where n_s is the saturation density.
- Since all of our parameter are uniformly distributed in the beginning, after constrained by astronomical quantities, the number of EoS can be explained as distribution. We use a Gaussian distribution to fit the green bars, and the result is plotted as the pink dashed line.
- The center value of fitting function is .

$$\langle \mu_0 \rangle = 1.03\text{GeV}$$

which corresponds to $1.88n_s$.

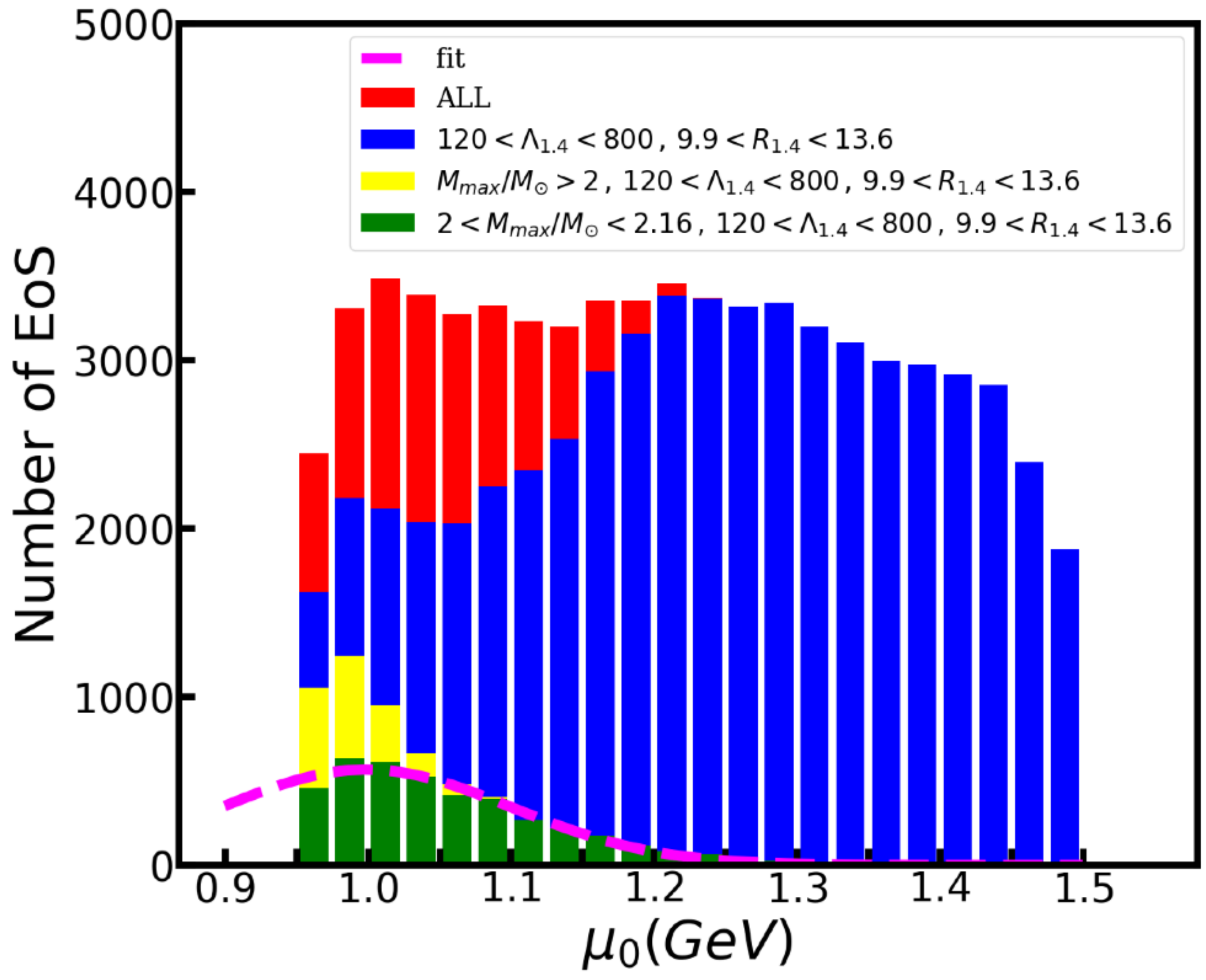

4. Numerical Results: PT chemical potential

● Next, we look through the chemical potential corresponding to the end of phase transition.

● The range of μ_1 does not change much when applying the tidal deformability and radius constraints.

● The lower boundary of maximum mass sets the upper and lower limit of μ_1.

● The upper boundary of maximum mass further sets the lower limit of μ_1.

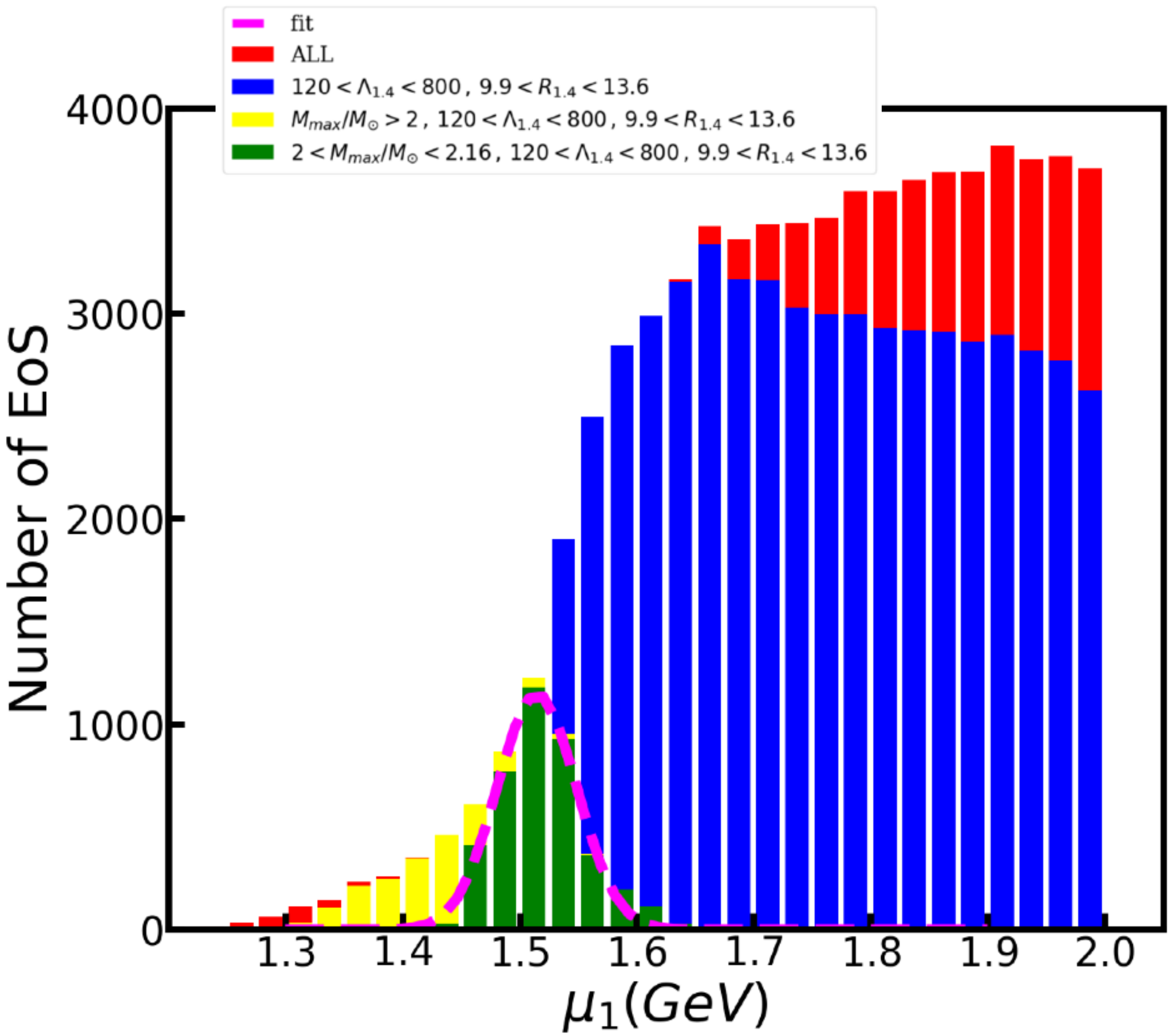

4. Numerical Results: PT chemical potential

- The range of μ_1 is:

$$1.42 \leq \mu_1 \leq 1.66\text{GeV}$$

and the corresponding range in baryon number density is:

$$6.06 \leq n_1/n_s \leq 11.37$$

- By fitting the green bars, we have the center value of the fitting function:

$$\langle \mu_1 \rangle = 1.51\text{GeV}$$

and the corresponding baryon number density is $7.87n_s$.

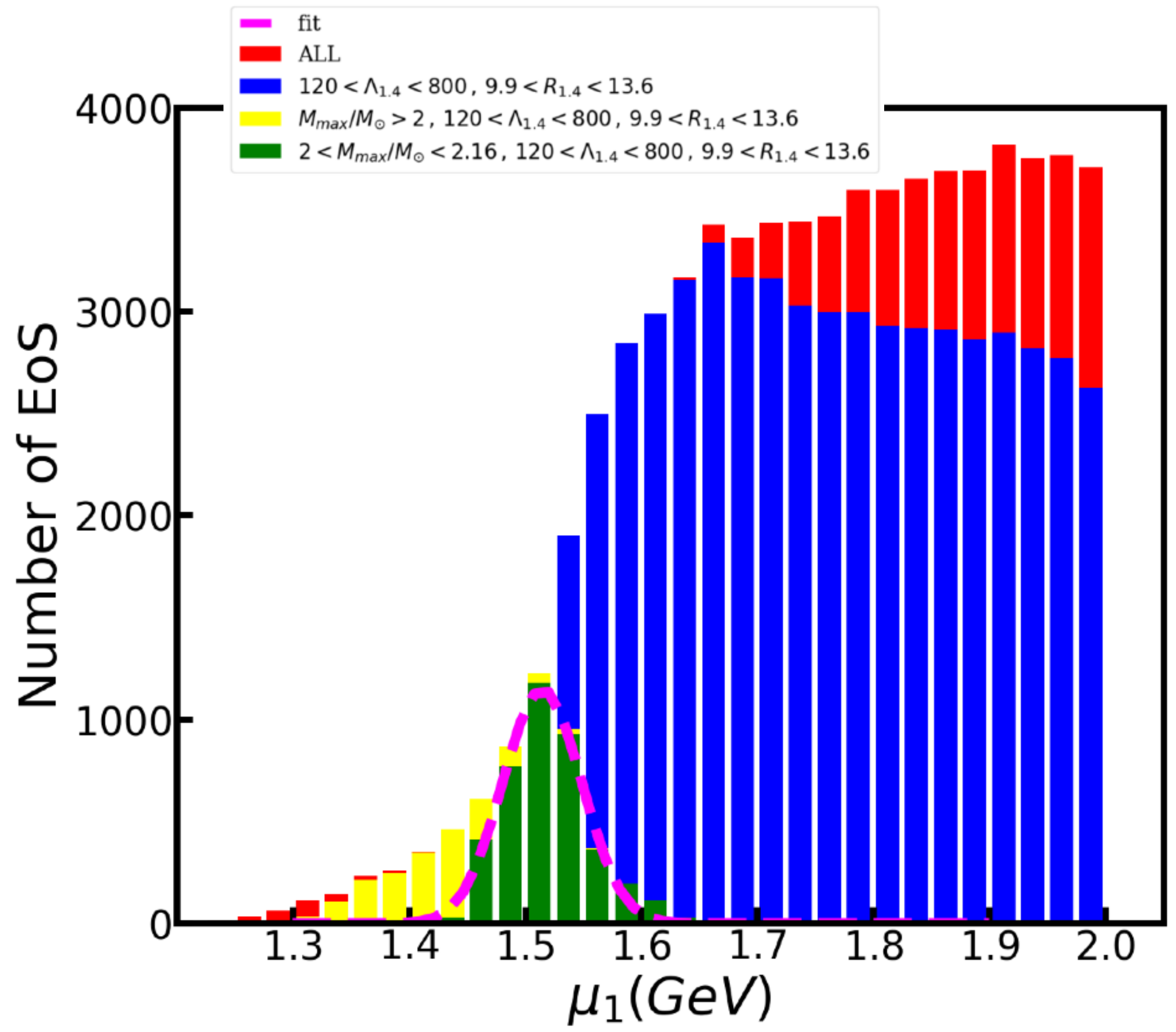

4. Numerical Results: various constraint conditions

- The appearance of hyperons reduces upper limit μ_0.

Astronomical Observation			Parameter Restriction										
M_{max}	$\Lambda_{1.4}$	$R_{1.4}$		μ_{0max}	n_{0max}	$\langle\mu_0\rangle$	$\langle n_0\rangle$	μ_{1min}	μ_{1max}	n_{1min}	n_{1max}	$\langle\mu_1\rangle$	$\langle n_1\rangle$
2-2.16	120-800	9.9-13.6	Nq	1.32	4.11	1.03	1.88	1.42	1.66	6.06	11.37	1.51	7.87
			NYq	1.12	3.16	1.01	1.64	1.42	1.65	6.13	11.14	1.53	8.22
2-2.35	120-800	9.9-13.6	Nq	1.32	4.11	1.00	1.57	1.31	1.66	4.57	11.36	1.50	7.64
			NYq	1.12	3.16	0.99	1.38	1.31	1.65	4.56	11.14	1.50	7.59
2-2.16	344-800	9.9-13.6	Nq	1.32	4.11	1.08	2.39	1.42	1.58	6.06	9.25	1.50	7.62
			NYq	1.05	2.31	0.99	1.35	1.42	1.59	6.13	9.52	1.49	7.39
2-2.16	120-800	10.62-12.83	Nq	1.32	4.11	1.04	1.99	1.42	1.61	6.06	10.13	1.51	7.84
			NYq	1.12	3.16	1.01	1.63	1.42	1.63	6.13	10.72	1.52	8.07
2-2.16	344-580	10.62-12.83	Nq	1.32	4.11	1.08	2.39	1.42	1.58	6.06	9.24	1.50	7.62
			NYq	1.05	2.31	0.99	1.39	1.44	1.59	6.40	9.52	1.49	7.43

4. Numerical Results: various constraint conditions

- The upper limit of maximum mass sets the lower limit of μ_1.

Astronomical Observation			Parameter Restriction										
M_{max}	$\Lambda_{1.4}$	$R_{1.4}$		μ_{0max}	n_{0max}	$\langle\mu_0\rangle$	$\langle n_0\rangle$	μ_{1min}	μ_{1max}	n_{1min}	n_{1max}	$\langle\mu_1\rangle$	$\langle n_1\rangle$
2-2.16	120-800	9.9-13.6	Nq	1.32	4.11	1.03	1.88	1.42	1.66	6.06	11.37	1.51	7.87
			NYq	1.12	3.16	1.01	1.64	1.42	1.65	6.13	11.14	1.53	8.22
2-2.35	120-800	9.9-13.6	Nq	1.32	4.11	1.00	1.57	1.31	1.66	4.57	11.36	1.50	7.64
			NYq	1.12	3.16	0.99	1.38	1.31	1.65	4.56	11.14	1.50	7.59
2-2.16	344-800	9.9-13.6	Nq	1.32	4.11	1.08	2.39	1.42	1.58	6.06	9.25	1.50	7.62
			NYq	1.05	2.31	0.99	1.35	1.42	1.59	6.13	9.52	1.49	7.39
2-2.16	120-800	10.62-12.83	Nq	1.32	4.11	1.04	1.99	1.42	1.61	6.06	10.13	1.51	7.84
			NYq	1.12	3.16	1.01	1.63	1.42	1.63	6.13	10.72	1.52	8.07
2-2.16	344-580	10.62-12.83	Nq	1.32	4.11	1.08	2.39	1.42	1.58	6.06	9.24	1.50	7.62
			NYq	1.05	2.31	0.99	1.39	1.44	1.59	6.40	9.52	1.49	7.43

4. Numerical Results: various constraint conditions

- The lower limit of tidal deformability changes the upper limit of μ_1.

Astronomical Observation			Parameter Restriction										
M_{max}	$\Lambda_{1.4}$	$R_{1.4}$		μ_{0max}	n_{0max}	$\langle\mu_0\rangle$	$\langle n_0\rangle$	μ_{1min}	μ_{1max}	n_{1min}	n_{1max}	$\langle\mu_1\rangle$	$\langle n_1\rangle$
2-2.16	120-800	9.9-13.6	Nq	1.32	4.11	1.03	1.88	1.42	1.66	6.06	11.37	1.51	7.87
			NYq	1.12	3.16	1.01	1.64	1.42	1.65	6.13	11.14	1.53	8.22
2-2.35	120-800	9.9-13.6	Nq	1.32	4.11	1.00	1.57	1.31	1.66	4.57	11.36	1.50	7.64
			NYq	1.12	3.16	0.99	1.38	1.31	1.65	4.56	11.14	1.50	7.59
2-2.16	344-800	9.9-13.6	Nq	1.32	4.11	1.08	2.39	1.42	1.58	6.06	9.25	1.50	7.62
			NYq	1.05	2.31	0.99	1.35	1.42	1.59	6.13	9.52	1.49	7.39
2-2.16	120-800	10.62-12.83	Nq	1.32	4.11	1.04	1.99	1.42	1.61	6.06	10.13	1.51	7.84
			NYq	1.12	3.16	1.01	1.63	1.42	1.63	6.13	10.72	1.52	8.07
2-2.16	344-580	10.62-12.83	Nq	1.32	4.11	1.08	2.39	1.42	1.58	6.06	9.24	1.50	7.62
			NYq	1.05	2.31	0.99	1.39	1.44	1.59	6.40	9.52	1.49	7.43

4. Numerical Results: various constraint conditions

- The radius constraints is loose.

Astronomical Observation			Parameter Restriction											
M_{max}	$\Lambda_{1.4}$	$R_{1.4}$		μ_{0max}	n_{0max}	$\langle\mu_0\rangle$	$\langle n_0\rangle$	μ_{1min}	μ_{1max}	n_{1min}	n_{1max}	$\langle\mu_1\rangle$	$\langle n_1\rangle$
2-2.16	120-800	9.9-13.6	Nq	1.32	4.11	1.03	1.88	1.42	1.66	6.06	11.37	1.51	7.87
			NYq	1.12	3.16	1.01	1.64	1.42	1.65	6.13	11.14	1.53	8.22
2-2.35	120-800	9.9-13.6	Nq	1.32	4.11	1.00	1.57	1.31	1.66	4.57	11.36	1.50	7.64
			NYq	1.12	3.16	0.99	1.38	1.31	1.65	4.56	11.14	1.50	7.59
2-2.16	344-800	9.9-13.6	Nq	1.32	4.11	1.08	2.39	1.42	1.58	6.06	9.25	1.50	7.62
			NYq	1.05	2.31	0.99	1.35	1.42	1.59	6.13	9.52	1.49	7.39
2-2.16	120-800	10.62-12.83	Nq	1.32	4.11	1.04	1.99	1.42	1.61	6.06	10.13	1.51	7.84
			NYq	1.12	3.16	1.01	1.63	1.42	1.63	6.13	10.72	1.52	8.07
2-2.16	344-580	10.62-12.83	Nq	1.32	4.11	1.08	2.39	1.42	1.58	6.06	9.24	1.50	7.62
			NYq	1.05	2.31	0.99	1.39	1.44	1.59	6.40	9.52	1.49	7.43

4. Numerical Results: various constraint conditions

- After applying the most strict constraints, the most probable phase transition region is:

$$0.99 \leq \mu_B \leq 1.49\text{GeV} \qquad 1.39 \leq n_B/n_s \leq 7.43$$

Astronomical Observation			Parameter Restriction										
M_{max}	$\Lambda_{1.4}$	$R_{1.4}$		μ_{0max}	n_{0max}	$\langle\mu_0\rangle$	$\langle n_0\rangle$	μ_{1min}	μ_{1max}	n_{1min}	n_{1max}	$\langle\mu_1\rangle$	$\langle n_1\rangle$
2-2.16	120-800	9.9-13.6	Nq	1.32	4.11	1.03	1.88	1.42	1.66	6.06	11.37	1.51	7.87
			NYq	1.12	3.16	1.01	1.64	1.42	1.65	6.13	11.14	1.53	8.22
2-2.35	120-800	9.9-13.6	Nq	1.32	4.11	1.00	1.57	1.31	1.66	4.57	11.36	1.50	7.64
			NYq	1.12	3.16	0.99	1.38	1.31	1.65	4.56	11.14	1.50	7.59
2-2.16	344-800	9.9-13.6	Nq	1.32	4.11	1.08	2.39	1.42	1.58	6.06	9.25	1.50	7.62
			NYq	1.05	2.31	0.99	1.35	1.42	1.59	6.13	9.52	1.49	7.39
2-2.16	120-800	10.62-12.83	Nq	1.32	4.11	1.04	1.99	1.42	1.61	6.06	10.13	1.51	7.84
			NYq	1.12	3.16	1.01	1.63	1.42	1.63	6.13	10.72	1.52	8.07
2-2.16	344-580	10.62-12.83	Nq	1.32	4.11	1.08	2.39	1.42	1.58	6.06	9.24	1.50	7.62
			NYq	1.05	2.31	0.99	1.39	1.44	1.59	6.40	9.52	1.49	7.43

5. Summary

Thank You!

● We use the sound speed interpolation to construct the EoS of hybrid star. The sound speed interpolation can consider the first-order phase transition while avoiding using hadron and quark model in the phase transition region where they are unreliable.

● For hadron matter, we use relativistic mean field theory. For quark matter, we use the Dyson-Schwinger equation approach.

● We construct the EoS with different parameters, and use astronomical observables(mass, radius and tidal deformability of neutron star) to constrain the range of parameters.

● We constrain the range of the phase transition chemical potential, and calculated the most probable value of the phase transition.

● Among the astronomical constraints, the upper bounds of maximum mass and lower bounds of tidal deformability are very important in constraining the parameters. The range of radius is a loose constraints, but since the mass, tidal deformability and radius are correlated, when the radius range is small enough, it will also provides strong constraints on the range of the phase transition region.